Aalborg University

Masters Thesis
by Jakob Aagaard Lükensmejer Pedersen

INVESTIGATING IF OSMOTIC EFFECTS EXPLAIN THE INFLUENCE OF SODIUM CHLORIDE UPON THE FILTRATION CHARACTERISTICS OF POLYACRYLIC ACID

Supervisor:
Morten Lykkegaard Christensen

Date:
Friday 10th June, 2016

Det Teknisk-Naturvidenskabelige Fakultet
Kemiteknologi
Frederik Bajers Vej 7H
Phone 99 40 36 05
www.bio.aau.dk

Title:
Investigating if Osmotic Effects Explain the Influence of Sodium Chloride Upon the Filtration Characteristics of Polyacrylic Acid

Project period:
1 Sep. 2015 - 10 Jun. 2016

Author:
Jakob Aagaard Lükensmejer Pedersen

Supervisor:
Morten Lykkegaard Christensen

Abstract:

A subject of much research is how fouling occur in membrane bioreactors (MBR). Authors in literature have documented that extracellular polymeric substances (EPS), present in sludge, contain various charged groups that causes counterions to be present. These counterions have previously been shown to be causing colligative properties to arise in sludge, such as osmotic pressure. In this study we attempt to illuminate some aspects of how colligative properties in a filter cake may influence a filtration scenario. Filtration experiments were performed with a filter cake consisting of polyacrylic acid (PAA), while varying the concentration of sodium chloride. It was found that the filtration resistance of the filter cake was being reduced by an increase in salt concentration. The reduction in filtration resistance occurred despite the filter cake is expected to be more compressed at higher salt concentrations, which would typically be expected to result in a higher hydrauilic resistance to flow. A simple model for the osmotic pressure of a polyelectrolyte gel, based on Donnan-equilibria, predicted that the osmotic pressure of the gel should decrease with an increase in salt concentration. Osmotic pressure of the filter cake was therefore found to be a plausible cause for the observed relation between filtration resistance and salt concentration.
The filter cake was found to be compressible at low salt concentrations, but the compressibility decreased with an increase in salt concentration. A plausible cause for this phenomena was also found to be osmotic pressure of the filter cake layer. A reduction in filter cake osmotic pressure is expected to cause deswelling of the filter cake. The decrease of the filter cake compressibility may be due to the filter cake deswelling at higher salt concentrations, meaning it may not easily compress further.

Resume

Et emne der har fået meget interesse i litteraturen, er hvordan fouling foregår i membran bioreaktorer (MBR). I litteraturen er det blevet dokumenteret at ekstracellulære polymeriske substanser (EPS), der er tilstede i slam, indeholder forskellige ladede kemiske grupper der er årsag til tilstedeværelse af modioner. Disse modioner er tidligere blevet vist at forårsage kolligative egenskaber i slam, såsom osmotisk tryk. I dette studie vil vi forsøge at forklare nogle aspekter af hvordan kolligative egenskaber i en filterkage kan påvirke et filtrationsscenarie. Filtrationseksperimenter blev foretaget med en filterkage bestående af polyakrylsyre (PAA), mens koncentrationen af natriumklorid blev ændret. Vi fandt at filtrationsmodstanden af filterkagen blev reduceret når saltkoncentrationen blev øget. Denne reduktion af filtrationsmodstand skete på trods af at filterkagen forventes at være mere sammentrykket ved højere saltkoncentrationer, hvilket typisk ville være forbundet med en større hydraulisk modstand mod flow. En simpel model for osmotisk tryk af en polyelectrolyt gel, basered på Donnan-ligevægte, forudså at osmotisk tryk af gelen skulle falde når saltkoncentrationen øgedes. Osmotisk tryk af filterkagen blev derfor fundet til at være en mulig årsag til den observerede relation mellem filtrationsmodstand og saltkoncentration.

Filterkagen viste sig at være kompressibel ved lave saltkoncentrationer, men kompressibiliteten faldt når saltkoncentrationen øgedes. En mulig årsag til dette fænomen kunne også være osmotisk tryk i filterkagen. En reduktion i filterkagens osmotisk tryk forventes at forårsage at filterkagen kan suge mindre vand, og derfor bliver mere kompakt. Faldet i filterkagens kompressibilitet kunne skyldes at filterkagen kompakteres ved højere saltkoncentrationer, og derfor er mindre tilbøjelig til at kompakteres yderligere.

Preface

This Master's thesis was written by Jakob Aagaard Lükensmejer Pedersen on his 9^{th} and 10^{th} semester of Chemical Engineering at Aalborg University, and handed in the summer of 2016.

Citations are made as [Author(s) Year] and are placed immediately prior to a dot if the citation refers to the sentence. If a citation is directly referred to in the text, the citation appears as a Author [year].

The bibliography is listed in alphabetical order.

Appendices

Appendix A: Piston system program
Appendix B: Continuous system program
Appendix C: The continuous setup
Appendix D: Membrane filtration resistance

Abbreviations

Abbreviation	Name
MBR	Membrane bioreactor
EPS	Extracellular polymeric substances
PAA	Polyacrylic acid
PAA450kDa	Polyacrylic acid, MW 450 kDa
PAA3MDa	Polyacrylic acid, MW 3 MDa
R_t	Total filtration resistance
R_t^{app}	Apparent total filtration resistance
α	Specific filtration resistance
α^{app}	Apparent specific filtration resistance
π	Osmotic pressure
π^{app}	Apparent osmotic pressure
ΔP	Transmembrane pressure
ΔP_c	Pressure drop across filter cake

Contents

Chapter 1 Introduction

Membrane bioreactors (MBR) are a promising technology for wastewater treatment that attracts attention in literature. One of the significant areas that are investigated, are the effects influencing the flux through the applied membranes.

Researchers have been attempting to illuminate the chemical nature of the sludge deposited on the membrane surface, which might make it possible to determine which mechanisms governs the filtration resistance. In perspective, a deeper understanding of the mechanisms involved, allows for a greater ability to optimize the processes.

When considering a filter cake layer created in membrane bioreactor, the filtration resistance is typically quite high, in the range of 10^{13} – 10^{14} [Lin et al. 2009; 2011, Ping Chu and Li 2005, Wang et al. 2007].

Zhang et al. [2013] argue that the high specific resistances observed cannot be fully explained by simple hydraulic resistance to flow, by applying the Carman-kozeny equation. Instead, they propose
that a significant contributor to the observed high filtration resistance may be arising from the negatively charged extracellular polymeric substances (EPS) present in sludge. EPS have previously been shown to exert colligative properties due to the presence of counterions to the negative charges [Keiding and Wybrand 2001]. The proposed mechanism for EPS influence in filtration, is that the counterions provide osmotic pressure in the filter cake layer, which is counteracting the applied transmembrane pressure, and thus reducing the flux [Keiding and Wybrand 2001, Zhang et al. 2013, Lin et al. 2014a].

1.1 The purpose of this project

This study will attempt to shed light on how osmotic effects in a filter cake layer, originating from the counterions of polyanionic polymers, may be of influence a filtration scenario.

The approach I will use includes performing filtrations upon polyacrylic acid, a simple anionic polymer, and documenting how the filtration characteristics is influenced by variations in system parameters, such as filtration pressure and sodium chloride concentration.

The collected data will be compared to a theoretic model in order to discuss if the observations can be explained by osmotic pressure of the filter cake layer.

Chapter 2 Theory

2.1 Filtration theory

When considering a simple filtration scenario, the Darcy equation is very useful, **Equation 2.1**.

$$J = \frac{\Delta P}{\mu * R_t} \qquad \textbf{(Equation 2.1)}$$

Where J is the flux ($\frac{m}{s}$), TMP is the filtration pressure (Pa), μ is the viscosity of the liquid ($Pa * s$) and R_t is the total filtration resistance (m^{-1}). In scenarios where there is a significant difference in dissolved substances, a difference in osmotic pressure between feed and permeate may be influential, and reduces the effective ΔP. In the simplest of scenarios, pure water is filtrated through a membrane, with the only filtration resistance arising from the membrane filtration resistance, R_m. If some material in the water is deposited on the membrane, we may utilize a specific filtration resistance for the material that is deposited, α in $\frac{m}{kg}$. Then the total filtration resistance may be estimated by **Equation 2.2**.

$$J = \frac{\Delta P - \Delta \pi}{\mu * (R_m + \alpha * \omega)} \qquad \textbf{(Equation 2.2)}$$

Where ω is the mass of filter cake per square meter $\frac{kg}{m^2}$ and π is the osmotic pressure difference between the feed and permeate.

If a filtration system exhibits both an osmotic pressure and a filtration resistance, one must know one of these values in order to estimate the other from the obtained flux. If osmotic pressure is influential in a filtration scenario, but is assumed not to be, any estimation of the filtration resistance will be higher than the real filtration resistance. This size of this apparent filtration resistance R_t^{app} will therefore be governed by both the osmotic pressure and the actual filtration resistance. Similarly, if the filter cake resistance is assumed to be 0, any estimation of the osmotic pressure π^{app}, will be greater than the actual osmotic pressure.

Whenever I discuss an R_t^{app} in this report, it is with this in mind, that the magnitude of R_t^{app} will be affected by both filtration resistance and osmotic pressure. Similarly, if the R_t^{app} is attempted to be converterted to α, α^{app} is found, which will also increase in magnitude if osmotic pressure is influential.

2.2 Extracellular polymeric substances (EPS)

Some cells excrete polymeric substances, which help produce a 3-dimensional matrix, fixating the cells to a certain location, or in a cluster, such as biofilms [Lin et al. 2014b]. Therefore EPS is a very broad definition, and what the structure and composition of EPS is, may vary broadly upon the organisms that creates it, and under what conditions they live. EPS is present in bio-

logical wastewater systems, as some organisms in such system produces EPS. [Sheng et al. 2010]

The structure of EPS varies broadly, but includes proteins, polysaccharides and humic substances, and many different chemical groups [Froelund et al. 1996, Liu and Fang 2003]. The chemical groups include carboxyl, phosphoric and hydroxyl groups [Lin et al. 2014b]. Many charged groups in EPS originate from proteins, due to the carboxylic acid groups in the amino acids glutamic acid and aspartic acid [Dignac et al. 1998, Chen et al. 2012]

2.3 Osmotic pressure arising from EPS counterions

Osmotic pressure of sludge has been a topic of quite widespread interest in literature. One of the main papers that sparked interest in the subject was Keiding and Wybrand [2001], in which the authors were able use models based on osmotic pressure of sludge occuring due to extracellular polymeric substances (EPS), to fit experimental data for several physical phenomena in sludge. The phenomena that could be described using their expressions included freezing point depression, drying rates and swelling of EPS.

Several authors have described the colligative properties of sludge with models based on the properties of EPS [Keiding and Wybrand 2001, Keiding and Rasmussen 2003, Chen et al. 2012, Curvers et al. 2011]. EPS contain many functional groups, including carboxyl and phosphoric groups, and are therefore negatively charged at neutral pH [Chen et al. 2012]. The presence of negative charges are causing counterions to be present. The concentration of counterions were by Keiding and Rasmussen [2003], Keiding and Wybrand [2001] and Zhang et al. [2013] estimated by **Equation 2.3**.

$$C_{counterions} = \sigma * \rho * \frac{1-\beta}{\beta} \qquad \textbf{(Equation 2.3)}$$

Where σ is the charge density per mass of solids, ρ is the solid density and β is the porosity of the filter cake layer. This method is a simple way of estimating the concentration of EPS counterions in sludge.

Keiding and Rasmussen [2003] argue that EPS, determined to have an average size of 50 kDa and a charge density of 1 $\frac{meq}{g}$, will therefore result in a counterion concentration about 50 times higher than the polymer concentration. As osmotic pressure closely relates to concentration, the authors conclude that the majority of the osmotic pressure and other colligative properties of sludge should originate from the EPS counterions. This conclusion is supported by several authors [Zhang et al. 2013, Curvers et al. 2009, Lin et al. 2014a, Chen et al. 2012].

The concept of the charge density of macromolecules being a major contributor to colligative properties of a solution has been observed in the study of gels [Fernandez-Nieves et al. 2000], supporting the theory that the charge density of sludge may very well govern the colligative properties observed.

2.4 The influence of counterions in filtration scenarios

Typically monoatomic ions are not expected to cause any osmotic pressure in filtration scenarios that employ MF/UF membranes.

The paper [Zhang et al. 2013], in which the authors suggest that they observe osmotic effects due counterions of polyanionic substances in MF/UF, has sparked comments that questions the ability of monoatomic ions to produce osmotic pressure in MF/UF [Yoon 2013].
However we may describe a possible origin of osmotic pressure in filtration scenarios using simple reasoning. We consider a simple sketch of a filtration of sludge, see **Figure 2.1**

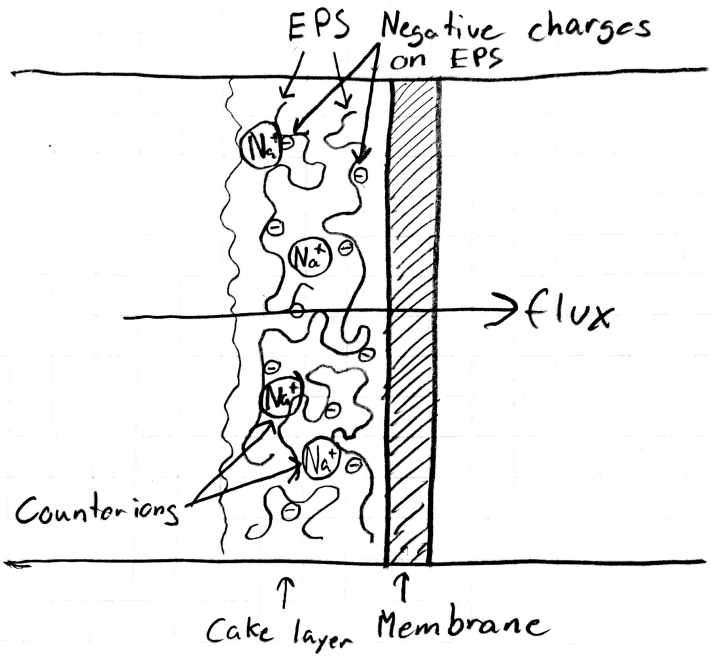

Figure 2.1: *Sketch of a cross-section of a cake filtration of sludge, with the filter cake containing negatively charged EPS, and is therefore associated with counterions*

During filtration, sludge flocs and other materials such as EPS are deposited on the membrane. Keiding and Wybrand [2001] suggest that the the EPS content will govern the colligative properties that it exhibits. The colligative properties will then be determined from the concentration of counter-ions to the EPS, which may be estimated by **Equation 2.3**. The degree to which this layer will exhibit osmotic properties, depends on the osmotic pressure of the surrounding liquids as well. As we are considering MF/UF filtration, we expect little to no difference in dissolved ions between the feed and the filtrate, which has also been experimentally confirmed [Keiding and Wybrand 2001].

In literature, **Equation 2.3** has been used to directly estimate the osmotic pressure of a filter cake layer, by using **Equation 2.4** while assuming the solution to be a dilute solution [Keiding and Rasmussen 2003].

$$\Delta\pi = C_{counterions} * R * T \qquad \textbf{(Equation 2.4)}$$

Filtrating liquid through the membrane will then require water to be expelled from the cake layer with a high osmotic pressure, to the permeate side with a lower osmotic pressure. This is expected to cause a drop in filtration pressure, reducing the permeate flux, as per Darcys law, $J = \frac{\Delta p - \Delta \pi}{R * \mu}$.

2.5 The influence of NaCl concentration upon osmotic pressure of a polyanionic cake layer

Several previous papers in literature have only considered a very simple relation between osmotic pressure and charge density of the EPS in sludge. Keiding and Rasmussen [2003] estimate the osmotic pressure differential between the filter cake and the permeate, by assuming that the counter ions in the filter cake is added to the concentration of ions in the permeate, by **Equation 2.3**.

Other papers have used a slightly different approach. Chen et al. [2012] use practically the same equation, **Equation 2.3**, except that they subtract the permeate ion concentration, conceptually illustrated on **Figure 2.2**.

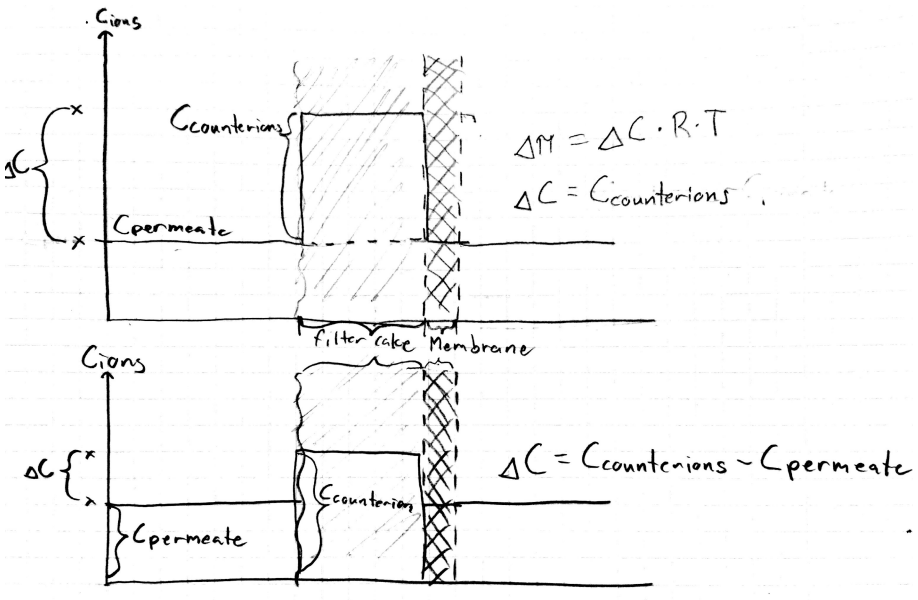

Figure 2.2: *Different approaches to estimate the osmotic pressure of a filter cake used in litterature. The upper image depicts the approach used by Keiding and Rasmussen [2003], where the osmotic pressure is estimated only from the concentration of counterions. the lower image depicts the approach used by Zhang et al. [2013] and Chen et al. [2012], where the osmotic pressure is estimated by the difference in concentration between the counterions and the permeate.*

However the actual mechanism whereby the osmotic pressure is generated by counterions, may be a little more complex. Curvers et al. [2009] mention that in a polymer gel system of polyelectrolytes, Donnan-equilibria governs the distribution of ions between the gel and the surrounding bulk. Considering that there has previously been drawn parallels between MBR filter cakes

and gels, Donnan-equilibria may be worth considering [Keiding and Rasmussen 2003, Legrand et al. 1998].

Consider a simple sketch of a MF/UF membrane surface with polyanionic polymers on the surface, and filtratring a sodium chloride solution through the membrane, see **Figure 2.3**.

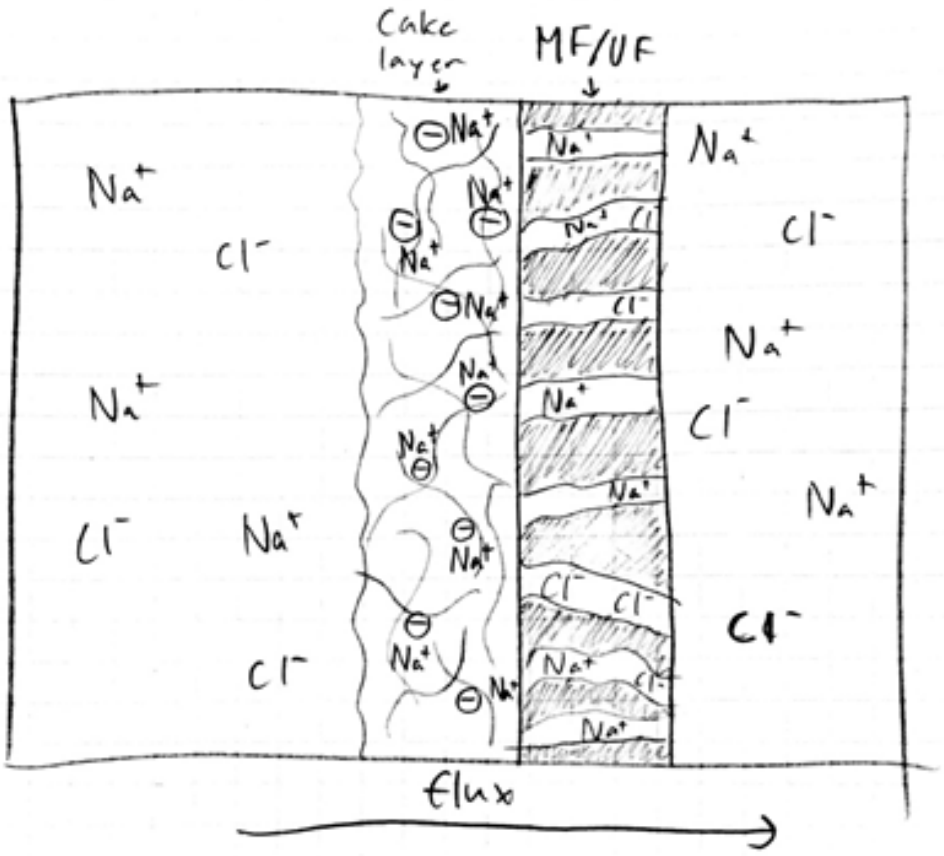

Figure 2.3: *Sketch of a surface of a MF/UF membrane with a cake layer of polyanionic polymers, through which a sodium chloride solution is being filtrated.*

In **Figure 2.3** a gel-like filter cake of polyanionic polymers is present on the surface of the membrane, resulting in a given charge density. As a solution of sodium chloride is filtrated through the membrane, dissolved ions associates with the negative charges of the filter cake.

In a system such as this, the distribution of ions can be estimated by applying Donnan equilibrium theory, assuming that the flux of water does not cause displacement from the Donnan equilibrium.
To do this, we consider two volumes separated by a semipermeable membrane. One volume is the cake layer containing impermeable anionic substanes, while the other side of the membrane is a bulk solution of infinite volume, see **Figure 2.4**.

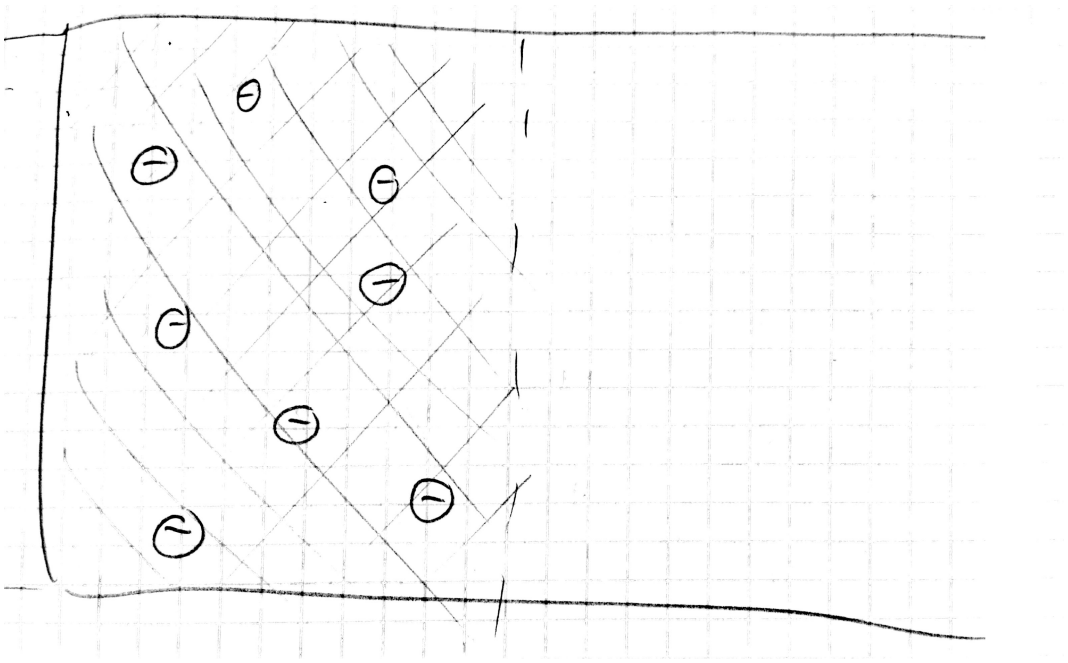

Figure 2.4: *A model for predicting the influence of monovalent salt concentration to the osmotic pressure of a gel layer. Negative charges fixed in a given volume, in liquid contact with an infinite bulk volume*

This model then allows us to apply Donnan equilibria by **Equation 2.5** to estimate the equilibrium concentration of ions in the cake layer [Chang and Kaplan 1977].

$$C^-_{in} * C^+_{in} = C^-_{out} * C^+_{out} \qquad \textbf{(Equation 2.5)}$$

Where C is the total molar concentration of negatively and positively charged permeable ions, respectively, on either side of the semipermeable membrane. As we assume that the volume of the surrounding solution (being the permeate and the bulk liquid) is significantly larger than the volume of the filter cake, we can consider the bulk concentration to be unaffected by the movement of ions. From now on we will refer to C_{in} as C_{gel} and C_{out} as C_{bulk}.
In this case, we are considering a system of dissolved sodium chloride and impermeable anionic substances, A^-, Na^+ and Cl^-. At equilibrium, the following equation should hold true.

$$Cl^-_{gel} * Na^+_{gel} = Cl^-_{bulk} * Na^+_{bulk} \qquad \textbf{(Equation 2.6)}$$

As the impermeable anionic substances are expected to be charge-neutralized by Na^+ ions (A^-_{gel}=Na^+_{gel}), we may use the following set of initial concentrations:

Table 2.1: Initial conditions applied for Donnan equilibrium calculations

Initial conditions

Ionic species	Inside	Outside
A^-	A^-_{gel}	0
Na^+	A^-_{gel}	Na^+_{bulk}
Cl^-	0	Cl^-_{bulk}

As the system reaches equilibrium, ions will move from the bulk liquid to the gel network. This will result in an certain increase (x) in the concentration of ions in the gel, while the bulk concentrations will remain unchanged, as we assume the bulk to be of infinite volume.

Table 2.2: equilibrium concentration applied for Donnan equilibrium calculations

Equilibrium concentrations

Ionic species	Inside	Outside
A^-	A^-_{gel}	0
Na^+	$A^-_{gel} + x$	Na^+_{bulk}
Cl^-	x	Cl^-_{bulk}

By using the description of concentrations given in **Table 2.2** in **Equation 2.6**, we may aquire the following equations.

$$x * (A^-_{gel} + x) = Cl^-_{bulk} * Na^+_{bulk} \qquad \textbf{(Equation 2.7)}$$

$$x^2 * A^-_{gel} * x - Cl^-_{bulk} * Na^+_{bulk} \qquad \textbf{(Equation 2.8)}$$

This is a quadratic equation that can be readily solved using the discriminant method, to yield the equilibrium concentrations in the gel network, as a function of charge concentration in the gel network, and bulk sodium chloride concentration.
The solution is given by:

$$x = \frac{-A^-_{gel} + \sqrt{A^-_{gel} - 4 * Cl^-_{bulk} * Na^+_{bulk}}}{2} \qquad \textbf{(Equation 2.9)}$$

Hereby the distribution of ions in the system illustrated in **Figure 2.3** has been obtained. As a Donnan-equilibrium distribution of ions will contribute to osmotic pressure, we may estimate the osmotic pressure of the system by considering the Donnan-equilibrium ion distribution [Chang and Kaplan 1977]. We do this by applying $\Delta\pi = \Delta C * R * T$ with **Table 2.2**, see **Equation 2.11**.

$$\Delta\pi = (\sum C_{gel} - \sum C_{bulk}) * RT \quad \textbf{(Equation 2.10)}$$

$$\Delta\pi = (x * (A^-_{gel} + x) - (Cl^-_{bulk} + Na^+_{bulk})) * RT \quad \textbf{(Equation 2.11)}$$

These calculations describes how the osmotic pressure differential between a gel and a bulk is influenced by changes in concentration of sodium chloride in the bulk and negative charges in the gel.

These equations describe how the osmotic pressure of the gel gradually decreases as the addition of monovalent ions suppresses the concentration difference due to the Donnan-effect, see **Figure 2.5**.

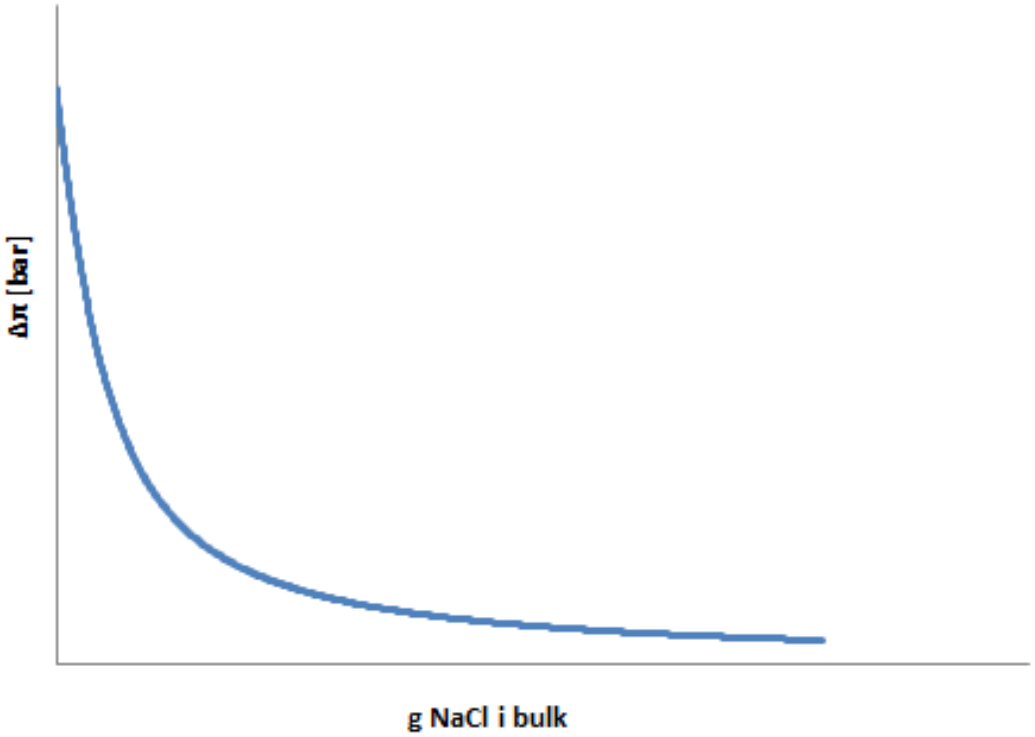

Figure 2.5: *An example of the general shape of the relation between osmotic pressure of a gel, and the concentration of salt in the bulk solution, calculated by Donnan-equilibria*

Noticeable assumptions required for applying these relations directly to describe the osmotic pressure of a filter cake in filtration scenarios include:

- Gel volume is unaffected by sodium chloride concentration
- The filtercake/gel reaches donnan equilibrium with the bulk
- The osmotic pressure arises solely from counterions, as the polymer itself provides negligible osmotic pressure [Keiding and Wybrand 2001].
- The solutions are dilute, so that the activity coefficient is 1.

Chapter 3 Materials and Method

For all experiments, a 0.22 μm polyethersulfone hydrophilic membrane from Merck Millipore, catalogue number GPWP14250, was used.
The polyacrylic acids (PAA) used were obtained by Sigma Aldrich, and had different molecular weights, which by the supplier was provided as a viscosity average molecular weight, M_v. The following PAA were used:

Abbreviation	M_v [Da]	Lot nr.	CAS	Supplier
PAA450kDa	450 000	04610EIV	9003-01-4	Sigma Aldrich
PAA3MDa	3 000 000	MKBS4532V	9003-01-4	Sigma Aldrich

3.1 Piston based deadend setup

A piston based deadend filtration unit, previously fabricated in our science department was applied, see **Figure 3.1** [Lorenzen et al. 2014].

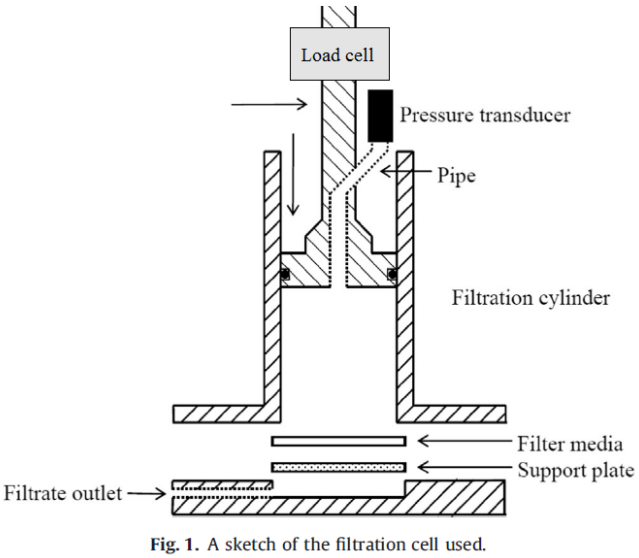

Fig. 1. A sketch of the filtration cell used.

Figure 3.1: *A sketch of the piston-deadend setup used from Lorenzen et al. [2014]*

The unit consist of a cylinder and piston with a diameter of 5 cm. The piston is terminated in a bottom plate, on which the membrane can be placed. The membrane is supported by a fine-meshed steel net, which is well supported to avoid any membrane warping. The piston position is controlled by stepper motors attached to threaded rods. The filtration pressure is measured by a load sensor, and maintained by software by controlling the piston position motors. Furthermore the piston is attached to a differential pressure sensor, which is logged by the software along with the filtration time, the piston position and the load sensor output.

3.1.1 Varying concentration of NaCl on PAA450kDa on piston setup

For all experiments in the piston based deadend setup, 10mg PAA450kDa was used. The GPWP14250 membranes from Merck Millipore were cut into fitting sizes, and installed in the

system with a circle of radius 2.5 cm of active filtration area.
The PAA450kDa solutions were prepared by making a 1 l stem solution of 2 $\frac{g}{l}$ of PAA450kDa. Also a 50 $\frac{g}{l}$ sodium chloride solution was prepared. 5 ml of the PAA450kDa stem solution (10 mg PAA450kDa) was along with the appropriate amount of sodium chloride solution, diluted to 100 ml and saved in a bluecap bottle for at least a day before each experiment, with the reasoning that the possible association of ions to the polymer might be a relatively slow process.

In total, the PAA450kDa solutions prepared, and their preparation and filtration parameters are described in **Table 3.1**.

Table 3.1: The filtrations performed on the piston deadend setup

Experiment ID	PAA [mg]	NaCl [$\frac{g}{l}$]	Volume [ml]	Membrane radius [cm]	Filtration Pressure [bar]
pistonPAA450kDa05NaCl	10	0.5	100	2.5	0.5
pistonPAA450kDa20NaCl	10	2.0	100	2.5	0.5
pistonPAA450kDa40NaCl	10	4.0	100	2.5	0.5
pistonPAA450kDa80$_1$NaCl	10	8.0	100	2.5	0.5
pistonPAA450kDa80$_2$NaCl	10	8.0	100	2.5	0.5
pistonPAA450kDa160NaCl	10	16.0	100	2.5	0.5

The general idea with these experiments were to create a filter cake of PAA on the membranes, and determine the filtration resistance through this filter cake as a function of various parameters. Pilot experiments determined that there were some time-dependent effects, so the following procedure was produced:

Table 3.2: The procedure used for experiments on the piston based deadend setup

Filtration type	Amount of filtrations	Repetitions	Notes
Procedure step	Waterflux	5-12	Performed at different filtration pressures
1	Deposition of 10 mg of PAA450kDa	1	The Rt of these experiments are not determined accurately
2	Cake filtration	6-15	
3	Overnight waiting		The membrane was left with 100 ml NaCl solution overnight
4	Cake filtration	6-30	

After each experiment, the filtration cylinder was refilled with new filtration solution, by tipping the cylinder about 45-60 degrees, and slowly pouring the solution down the side and into the cylinder.
The waterflux, the deposition solution and the water used in cake filtration were all adjusted

to the sodium chloride content of the individual experiment series.

The data treatment is performed by a script written in MatLab. A summery of its function is explained in **Section 4.1**, and the full script can be found in **Appendix A**.

3.2 Continuous setup

The continuous setup was developed, and can be found more accurately described in **Section 4.2.1**. Images of the setup can be found in **Appendix C**.
The continuous setup maintains a constant filtration pressure by the use of a vertical cylinder, a pump and overflow outlets. The system contains a prechamber, prior to the membrane housing, that allows for dosing PAA onto the membrane early in the filtration. The permeate flow is measured using a weight attached to a datalogger.

Prior to any experiment on the continuous setup, the demineralized water that was to be used in the experiment, was filtered through a 0.22 μm polyethersulfone hydrophilic membrane from Merck Millipore, catalogue number GPWP14250. 25 l of demineralized water was contained in 32 l buckets with lids, made from food-grade plastic, and roughly measured to 25 l using a water level indicator on the side of the bucket. The 25 l of demineralized water was conditioned to the feed parameters required for the individual experiments by pouring in a concentrated solution of the appropriate contents. The membrane applied was the same 0.22 μm Merck Millipore membrane, here mounted in a membrane housing (Advantec polypropylene 4.7 mm filter holder, catalogue number 43303020) with a circular active filtration area with a radius of 2.1 cm
The prechamber was filled with the PAA dosage solution, which contained a certain amount of PAA in a given volume, and all with a sodium chloride concentration of 0.5 $\frac{g}{l}$. Hereafter the water column cylinder was filled with the feed water to the specified water level. Water was slowly let into the prechamber, to reduce mixing. Once pressure was equalized throughout the system, the membrane outlet was opened and the datalogger started.

3.2.1 Varying concentration of NaCl on PAA450kDa on continuous setup

For these experiments, the prechamber was filled with 800 ml of dosage solution with 0.5 $\frac{g}{l}$ NaCl and 7.5 mg PAA450kDa. Some of the fittings in the system were not stainless steel, and iron oxide seemed to be generated in the system. The experiments were performed with variations in sodium chloride concentration in the feed (the 25 l bucket), using NaCl koncentrations: 0.5, 1.0, 2.0, 4.0 and 6.0 $\frac{g}{l}$.
The filtration pressure was obtained by 225 cm of water column.
The dosage solutions were prepared by mixing 800 ml of demineralized water with 8 ml of a 50 $\frac{g}{l}$ NaCl solution, and 3.75 ml of a 2 $\frac{g}{l}$ PAA450kDa solution. The dosage solution was mixed immediately prior to being deployed in the prechamber.

3.2.2 Varying mass of PAA3MDa on continuous setup

For these experiments, the prechamber was filled with 300 ml of dosage solution with 0.5 $\frac{g}{l}$ NaCl and the appropriate amount of PAA3MDa. The issue with iron oxide had been solved, by

applying plastic fittings instead. The experiments were performed with a constant concentration of 0.5 $\frac{g}{l}$ NaCl in the feed. Experiments were made with variations in the mass of PAA3MDa applied, using 0.1, 0.5, 1.0, 1.5, 2.0 and 7.5 mg of PAA3MDa.
The filtration pressure was obtained by 225 cm of water column.
The dosage solutions were prepared by mixing 300 ml of demineralized water with 3 ml of a 50 $\frac{g}{l}$ NaCl solution, and the appropriate amount of a 0.1 $\frac{mg}{ml}$ PAA3MDa solution. The dosage solution was mixed immediately prior to being deployed in the prechamber.

3.2.3 Varying concentration of NaCl on PAA3MDa on continuous setup

For these experiments, the prechamber was filled with 300 ml of dosage solution with 0.5 $\frac{g}{l}$ NaCl and 1.0 mg PAA3MDa. The issue with iron oxide had been solved, by applying plastic fittings instead. The experiments were performed with variations in sodium chloride concentration in the feed (the 25 l bucket), using NaCl koncentrations: 0.2, 0.5, 1.0, 2.0, 4.0 and 6.0 $\frac{g}{l}$.
The filtration pressure was obtained by 225 cm of water column for 24 $hours$ after the initiation of the experiment, then lowered to 75 cm for 12 $hours$ and then raised back to 225 cm for another 12 $hours$.
The dosage solutions were prepared by mixing 300 ml of demineralized water with 3 ml of a 50 $\frac{g}{l}$ NaCl solution, and 10 ml of a 0.1 $\frac{g}{l}$ PAA3MDa solution. The dosage solution was mixed immediately prior to being deployed in the prechamber.

3.3 Titration analysis

Titrations were performed on an autotitrator. The titration procedure of a sample was completed by the following steps:

1. (If sample is a membrane) Cut the membrane into pieces of about 2 mm
2. Dilute sample to 20 ml by addition of 0.5 $\frac{g}{l}$ NaCl solution
3. Lower the pH to approximately 2.5 by addition of 0.01 M HCl solution
4. Perform titration by addition of 0.05 M NaOH solution

The concentration of the 0.05 M NaOH titration solutions was verified by using the KHP (potassium hydrogen phthalate) method. 2 ml of a 14.005 $\frac{g}{l}$ KHP solution was diluted with 18 ml of 0.5 $\frac{g}{l}$ NaCl solution. The sample was titrated with the 0.05 M NaOH solution, which yielded the following $\frac{\Delta pH}{\Delta V}(V)$ plot, **Figure 3.2**.

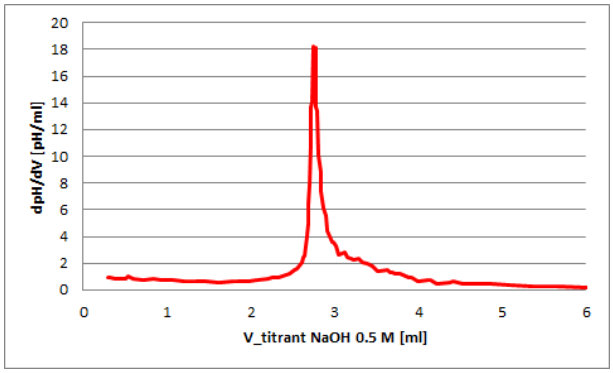

Figure 3.2: *The data from calibration of the titrant. Here the* $\frac{\Delta pH}{\Delta V}$ *is plotted over the volume of titrant used.*

The infliction point occured after 2.742 ml NaOH 0.5 M had been added. The amount of KHP in the sample was 0.13716 $mmol$, meaning the concentration of the NaOH was determined to be 0.05002 M. Because this deviation was so minor, the NaOH solution was assumed to be exactly 0.05 M.

The following titrations were performed:

- 20 mg PAA450kDa in solution
- 7.5 mg PAA450kDa in solution
- membrane from PAA450kDa20NaCl, in which 7.5 mg PAA450kDa had been used
- 1 mg PAA3MDa in solution
- membrane from PAA3MDa10NaCl, in which 1 mg PAA3MDa had been used

Chapter 4 Development and Verification of Experimental Method

Due to the amount of work that went into developing a prober experimental and technical method that was capable of producing consistent and accurate results, we have dedicated a section of this report to document the process.
This section will be a chronological tour through the design process of experiments, how the experiments where performed, and which conclusions could be drawn from the data. Most of the conclusions that can be obtained from the data in this chapter is either rather irrelevant for the project purpose, or covered more accurately and explicitly in **Section 5**.

4.1 Piston based deadend setup

4.1.1 Design of the experimental method

Initially, an experiment was developed to produce a filtration scenario that would be close to the the model system explained in **Section 2.5**, in which a filter cake layer of polyanionic substances is deposited on a membrane, and saline solutions filtrated through this cake.
Therefore a piston based dead-end filtration device (described in **Section 3.1**) was used to investigate the filtration resistance of PAA filter cakes under various NaCl concentrations. 0.22 μm polyethersulfone filters with 5 cm diameter were used while filtrating with 0.5 bars of pressure.
The filter cake was prepared by filtering 100 *ml* of a NaCl solution with 10 mg PAA450kDa through the membrane, see **Figure 4.1**. Subsequently the piston was reset, the chamber filled with NaCl solution, and then was filtered through the PAA450kDa filter cake, see **Figure 4.2**.

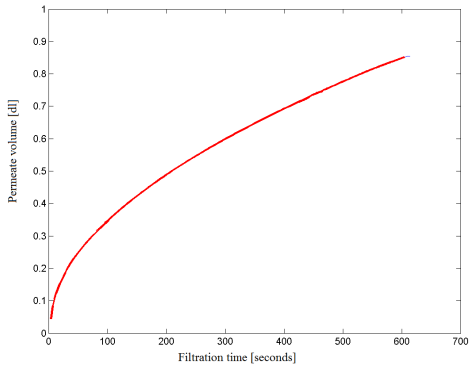

Figure 4.1: *An example of PAA450kDa being deposited on the membrane, here illustrated as the permate volume as a function of filtration time*

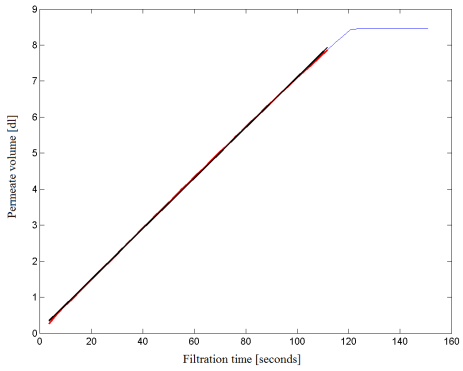

Figure 4.2: *An example of a NaCl solution being filtrated through a PAA450kDa filter cake, previously deposited on the membrane. The thin blue line is the original dataset. The red line is the range determined as the range of "active filtration" by an algorithm, and the black line is the linear fit to this data range, used for determining R_t^{app}. They are plotted as the permeate volume as a function of filtration time.*

Initial testing revealed that the R_t^{app} was changing during subsequent filtrations. As this might have been due to the newly formed gel-like layer having to reach equilibrium with the NaCl solution, the filtration cell was left overnight, and followed by filtrations the day after as well. Due to the nature of the collected data, an extensive MatLab function was developed **Appendix A**.
The MatLab function does the following:

- Loads raw data files and sorts them according to various identifying tags.
- Imports data from one filtration, identifies the filtration range, and performs a linear regression to estimate the total filtration resistance, and logs this resistance according to the identifying tags, see **Figure 4.1** and 4.2.
- For each NaCl solution, the R_t^{app} was plotted as a function of the filtration number, on the same PAA450kDa filter cake, see **Figure 4.3**.
- An algorithm identifies an approximate "plateau" for the R_t^{app}, and takes an average of these before and after the overnight equilibrium time, see **Figure 4.3**.
- The "plateau" R_t^{app} (and their associated deviations) is plotted over the NaCl concentration, see **Figure 4.4**.

4.1.2 PAA450k with variations in sodium chloride concentration

Using the procedure and the MatLab function of **Section 4.1.1**, we may examine a dataset of R_t^{app} of PAA450kDa, with varying NaCl concentrations, see **Figure 4.3**.

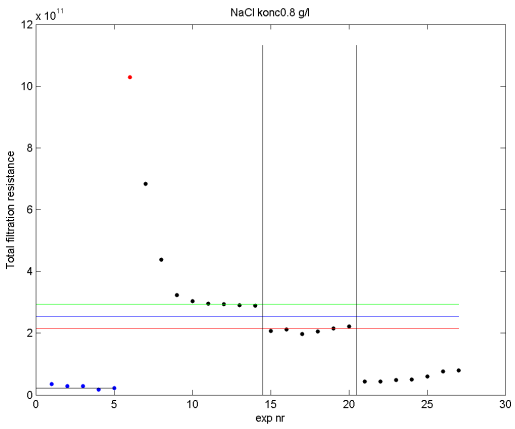

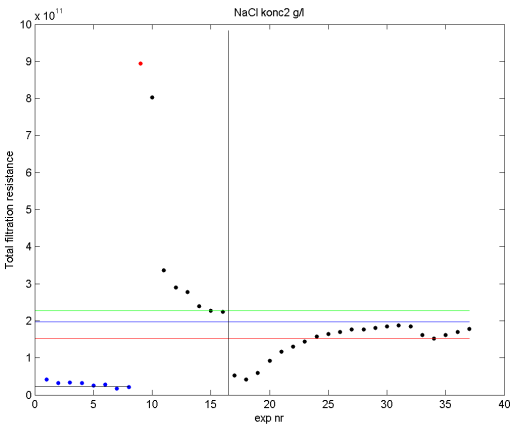

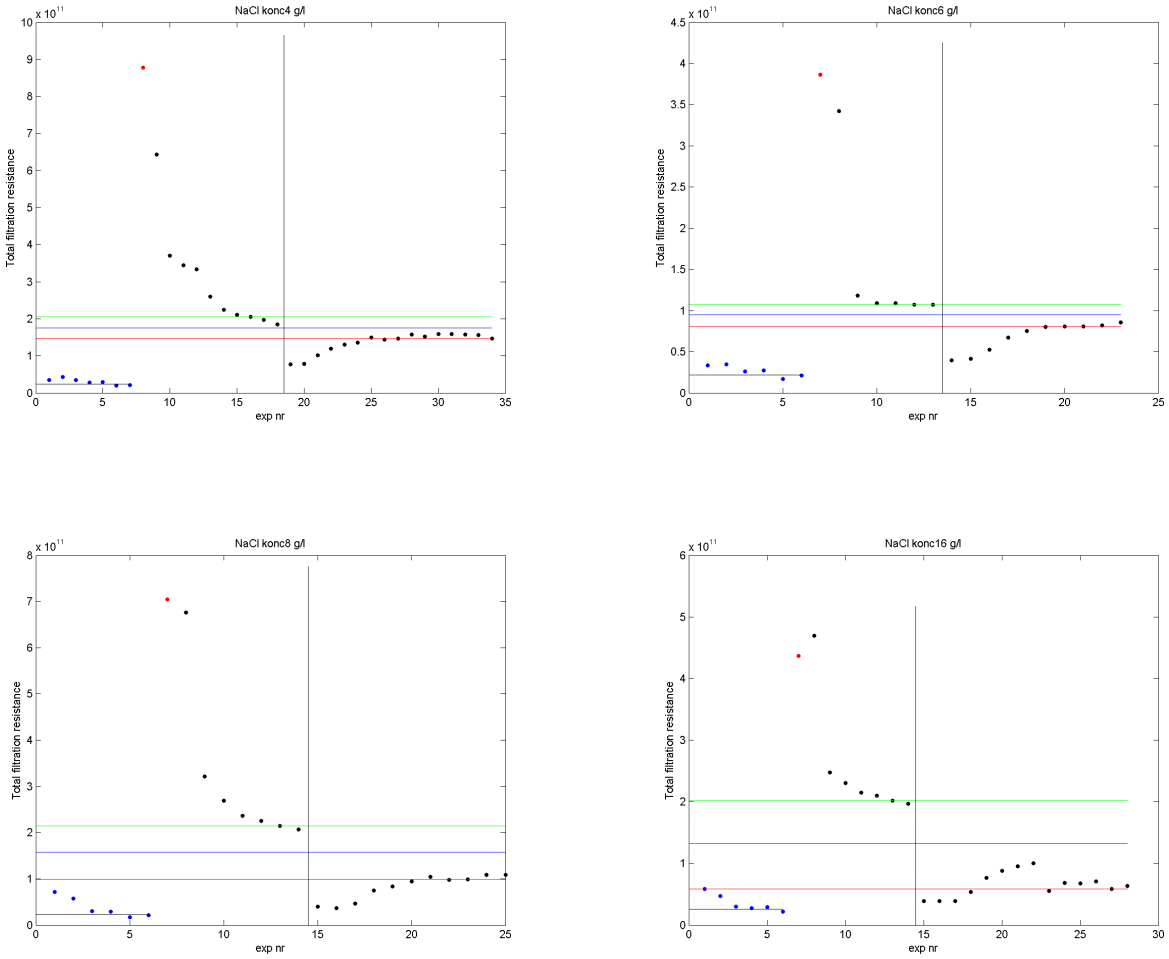

Figure 4.3: The data obtained on the piston setup for variations in NaCl concentration in the water being filtrated through a PAA450kDa filter cake. the vertical axis is the R_t^{app} obtained, plotted for each subsequent filtration through the same filter cake, seen on the horizontal axis. For each figure, the initial blue dots are a few test of the membrane filtration resistance. The single red dot it the experiment in which the PAA450kDa was deposited. The subsequent black dots are experiments of NaCl solutions being filtrated through the filter cake. The vertical black lines indicate that the system had been left overnight, while under no pressure. The horizontal blue, green and red lines are approximate average, max and min "plateau"-R_t^{app} determined by an algorithm. These R_t^{app} are plotted on **Figure 4.4**

Similar for these experiments are a very high initial R_t^{app} after PAA450kDa deposition, which quickly drops during subsequent filtrations. The R_t^{app} drops to a plateau. After the membrane is left overnight with 100 ml of NaCl solution, the R_t^{app} has dropped very low, but generally increases again to approach a plateau which is reasonably close to the plateau reached the day before.

The fact that the R_t^{app} decreases overnight followed by gradual increase to the same plateau-R_t^{app} as the day before, indicates that a reversible swelling process may be taking place.
The cause for the large initial drop in R_t^{app} is unknown, but is assumed to be due to some sort of adaptive process, occurring as PAA450kDa is forming a gel-like structure rather than being in solution. However leakage of PAA450kDa has not been excluded, and may be the underlying cause. Later experiments indicate that PAA450kDa leakage through the membrane may indeed be the cause for this behaviour.

If we take the plateau-R_t^{app} and plot that as a function of NaCl concentration applied, we get **Figure 4.4**.

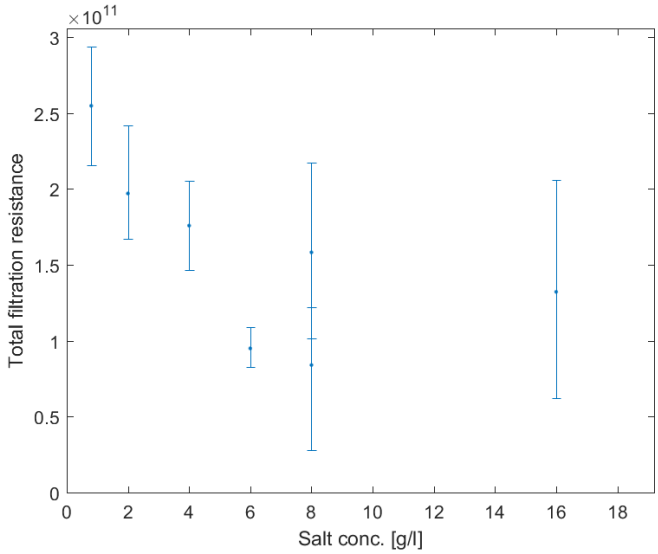

Figure 4.4: *The "plateau" R_t^{app} determined in **Figure 4.3** is plotted as a function of the NaCl concentration filtrated through the PAA450kDa filter cake*

As evident in **Figure 4.4**, plateau-R_t^{app} appears to decrease as NaCl concentration is increased. The general behaviour of the R_t^{app} as a function of the NaCl concentration appear similar to the change in osmotic pressure over NaCl concentration, as determined by the model in **Section 2.5**.

However, due to the rate of swelling being rapid enough to be influential in these batch piston deadend filtration experiments, and the rather large deviations in the data, we decided to produce a continuous deadend filtration setup.

4.2 Continuous deadend setup

4.2.1 Design of continuous setup

I designed a continuous setup so that it would be simple, versatile and accurate. The filtration pressure is obtained by a continuous column of water. A small chamber prior to the membrane housing allows for dosing PAA onto the membrane with the setup, while keeping the feed bucket/column and the PAA solution separate. The permeate flow is measured by a weight, and the data is logged to a pc.

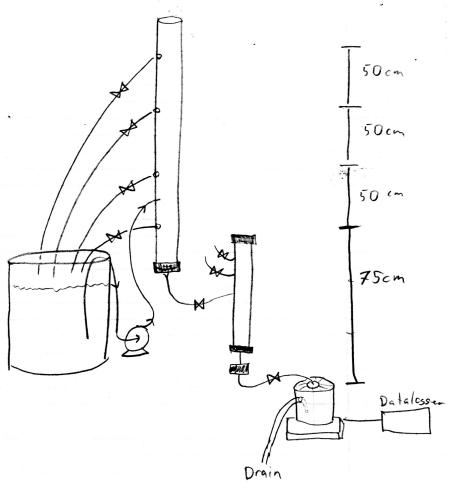

Figure 4.5: *A simple sketch of the continuous setup, found more explicitly drawn in* ***Appendix C****.*

The water column is maintaned by a pump connected to a feed bucket, and an overflow outlet, which leads excess water back to the feed bucket. The water column is contained within a 2.5 m acrylic pipe, in which we drilled outlets with 50cm interval, and attached valves to each one. In between of the water column and the membrane housing we added a smaller, airtight column to act as a 'dosage-chamber'. This would allow me to keep the PAA solution separated from the bulk of the feed, and deposit the PAA on the membrane rather early in the filtration, assuming somewhat linear flow through the 'dosage-chamber'. After the 'dosage-chamber', the membrane housing is attached, and the outlet is hanging over a bucket placed on a weight. The bucket is outfitted with an overflow outlet, which, when the water level reaches a critical height, is activated to act like a siphon and automatically empty the bucket again. Hereby the weight is able to act like a pseudo-continuous flow meter.

Pictures and sketches of the setup can be found in **Appendix C**.

For initial testing, we used filtration parameters close to what we used in the piston-based setup, being 10mg PAA450kDa in 800ml in the dosage chamber and the feed water was demineralized water with no added NaCl.
The raw weight output from the data log of this experiment over 7 days was converted to water volume, and can be seen on **Figure 4.6**.

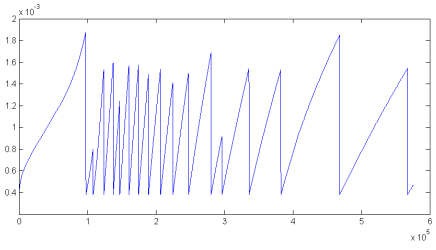

Figure 4.6: *An example of raw, untreated data from the setup. The vertical axis is the weights measurements in kg, and the horizontal axis is the elapsed filtration time in seconds. The weight gradually increases as permeate drips into the bucket. Once a critical water level is reached in the bucket, a siphon activates and empties the bucket.*

The data of **Figure 4.6** consist of areas where the weight gradually increases as permeate drips into the collection bucket. At some point, the water level reaches a threshold, at which

the overflow outlet begins to act like a siphon, and within a few minutes empties the bucket. Occasionally the siphon does not empty completely, meaning the siphon might activate at a lower water level.
In order to use these data properly, we need to convert it into the more useful data of cumulative permeate over time. We have achieved this by producing an algorithm which detects the points where the siphon activates and deactivates, and adds the weight to the data collected after the bucket has been emptied. In order to avoid having "dead-zones" in the data, as illustrated in **Figure 4.7**, we applied a simple linear interpolation to generate data in the time it takes the bucket to empty. The MatLab script can be examined in **Appendix B**.

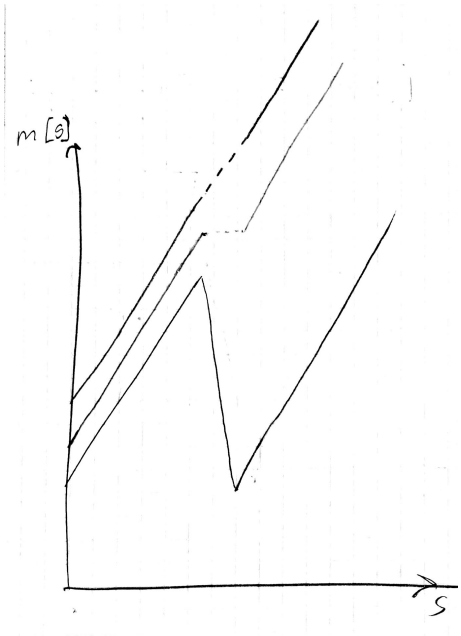

Figure 4.7: *A sketch of how the dataset of **Figure 4.6** was converted to cumulative permeate weight. An algorithm identifies the beginning and end of the siphoning stage, and fills the gap in the dataset by performing a linear interpolation.*

Doing so, we achieve a proper dataset of permeate volume over time, **Figure 4.8**. From here the dataset can be manipulated to give flux over time **Figure 4.9**, or plotting data over the permeate volume, as seen in **Figure 4.10**.

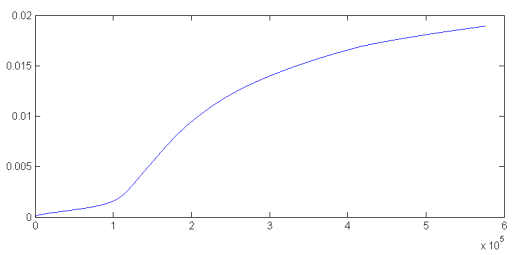

Figure 4.8: *Here the dataset of **Figure 4.6** was treated by the matlab script in **Appendix B**, and plotted as cumulative permeate volume in m^3 as a function of elapsed filtration time in seconds.*

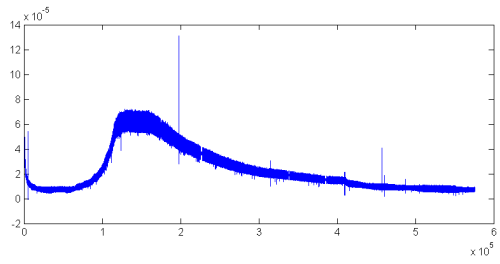

Figure 4.9: *Here the dataset of **Figure 4.6** was treated by the matlab script in **Appendix B**, and plotted as R_t^{app} in m^{-1} as a function of elapsed filtration time in seconds.*

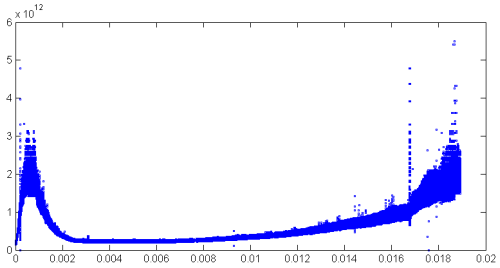

Figure 4.10: *Here the dataset of* ***Figure 4.6*** *was treated by the matlab script in* ***Appendix B****, and plotted as* R_t^{app} *in* m^{-1} *as a function of the cumulative permeate volume in* m^3*.*

Examining the data displayed on **Figure 4.10**, we can identify several characteristics. Initially the R_t^{app} increases as PAA450kDa is deposited on the membrane. after approximately 0.5-0.8 l permeate has been produced, a peak is observed. After the peak, the R_t^{app} gradually drops and reaches a plateau R_t^{app}, quite similar to what was observed on the piston deadend setup.

The plateau R_t^{app} reaches approximately $3.6{*}10^{11}$ m^{-1}, which is in a similar range to what was observed in **Figure 4.4**, although the filtration parameters are different, and the R_t^{app} can therefore not be directly compared.
After about 6 l of permeate has passed through the membrane, which is more than 2 days after the experiment was started, the R_t^{app} gradually increases higher than the plateau-R_t^{app}. The cause of this was examined and attempted to be avoided in the next section.

4.2.2 Attempts to avoid the gradual increase in filtration resistance

Especially two causes seem to be plausible explanations for this gradual increase in R_t^{app}., Bacterial growth may be fouling the membrane, or iron oxide being produced by exposed iron in the setup may cause some interference. We suspected iron oxide due to the color of the membrane after an experiment had been run with entirely colorless substances, see **Figure 4.11**.

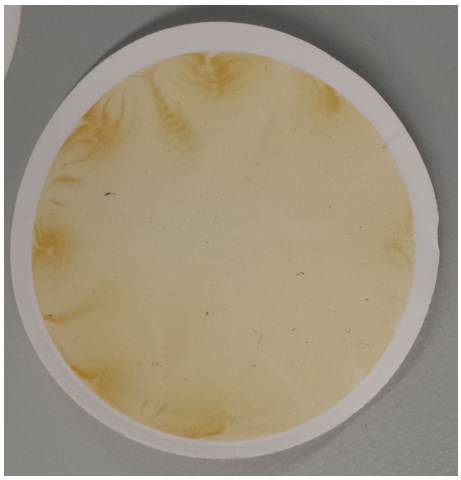

Figure 4.11: *The membrane after having been used in a early pilot experiment. The yellow color was most likely caused by iron oxide. The source of the iron oxide was later identified and replaced*

Unfortunately we did not identify the source of the iron oxide until later experiments, as it did stem from some not-quite-stainless steel fittings used in the setup. They were then replaced by

ABS (Acrylonitrile butadiene styrene) plastic fittings.
The other plausible cause would be bacterial growth. Consider E.Coli. as an example, they are typically considered to be 1x3 μm in size, and thus retained by the applied 0.22 μm pore size membrane [Reshes et al. 2008].

Considering the size of bacteria, the relatively large amount of water filtered and the time scale of the experiments, it is not unreasonable to consider that bacterial growth might occur and cause fouling of the membrane.

In order to avoid or at least limit possible fouling effects due to bacterial growth, new feed water containers were obtained and all demineralized water applied was filtered through the membranes prior to being applied in the filtration setup. Furthermore, new water was prepared before each experiment, and the experimental parameters were chosen so that most experiments could be completed within about two days.
Additionally, a few experiments were performed at increased pH, in another attempt to reduce bacterial growth. An experiment with the same parameters as used in the experiment on **Figure 4.10** was performed, but with the feed water being a 1.25 mM sodium hydroxide solution, with a pH of approximately 10, **Figure 4.12**.

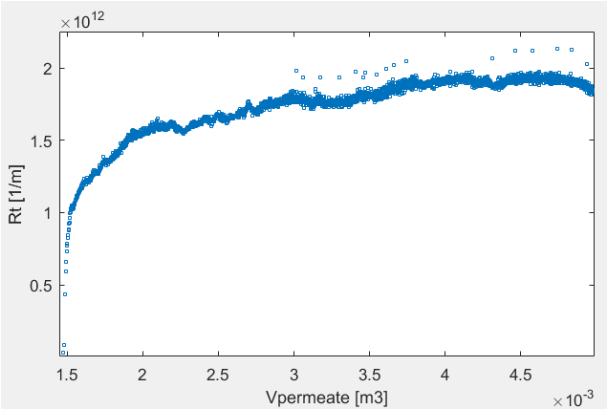

Figure 4.12: *Filtration of a 1.25 mM NaOH solution through a filter cake of 10 mg PAA450kDa. The higher pH appears to change the behaviour of PAA450kDa, as the R_t^{app} does not drop towards a "plateau".*

Interestingly, it appears that when filtrating PAA450kDa at a high pH, the R_t^{app} does not drop to a plateau R_t^{app} after the PAA deposition has completed, but rather behaves more simple and intuitive manner. Due to this simpler behaviour, it might be feasible to perform test of the influence of NaCl concentration at higher pH. However, because the higher R_t^{app} would result in very long experiments, we recreated the filtration parameters used in **Figure 4.12**, but with only a tenth of the PAA450kDa (1 mg), see **Figure 4.13** and 4.14.

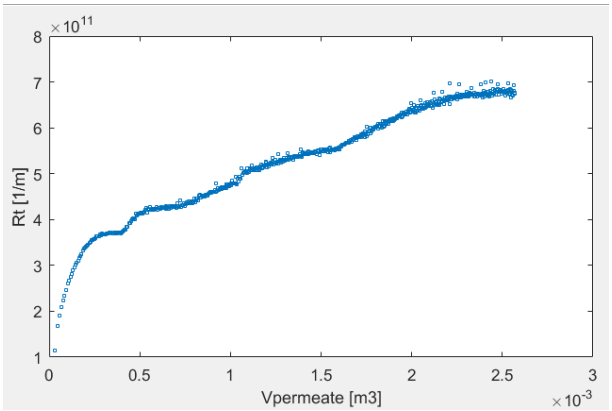

Figure 4.13: *Filtration of a 1.25 mM sodium hydroxide through a filter cake of 1 mg PAA450kDa.*

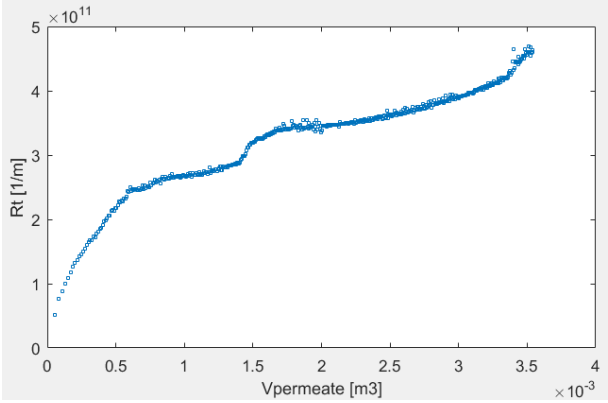

Figure 4.14: *(Filtration of a 5 mM sodium hydroxide through a filter cake of 1 mg PAA450kDa.*

Unfortunately the data for these experiments with 1 mg PAA450kDa were less convincing. The R_t^{app} continued to gradually increase, even after 1 l permeate had been produced, before which previous experiments revealed that almost all of the PAA450kDa should have been deposited. We cannot explain this effect, and we therefore decided to end further experiments with increased pH.

4.2.3 PAA450kDa with variations in sodium chloride concentration

These experiments were performed prior to the possible issue of iron oxide in the filtration system had been located and eliminated as explained in **Section 4.2.2**, which might have affected the results.
The experiments were performed with the system parameters as described in **Table 4.1**.

Table 4.1: A list of the experiments performed with a varying concentration of NaCl with PAA450kDa. $[NaCl]_{feed}$ is the feed concentration of NaCl, t is the elapsed time of the experiment, ΔP is the filtration pressure, V_{dose} is the prechamber volume of PAA3MDa solution used, $[\text{NaCl}]_{dose}$ is the NaCl concentration in the prechamber volume solution, m_{dose}^{PAA} is the mass of PAA3MDa dissolved in the dosage solution in the prechamber and ω is the expected mass of filter cake (PAA3MDa) per unit area.

Experiment ID	$[NaCl]_{feed}$	t	ΔP	V_{dose}	$[\text{NaCl}]_{dose}$	m_{dose}^{PAA}
PAA450kDa05NaCl	0.5 $\frac{g}{l}$	2 days	2.25 m H_2O	0.8 l	0.5 $\frac{g}{l}$	7.5 mg
PAA450kDa10NaCl	1.0 $\frac{g}{l}$	2 days	2.25 m H_2O	0.8 l	0.5 $\frac{g}{l}$	7.5 mg
PAA450kDa20NaCl	2.0 $\frac{g}{l}$	2 days	2.25 m H_2O	0.8 l	0.5 $\frac{g}{l}$	7.5 mg
PAA450kDa40NaCl	4.0 $\frac{g}{l}$	2 days	2.25 m H_2O	0.8 l	0.5 $\frac{g}{l}$	7.5 mg
PAA450kDa60NaCl	6.0 $\frac{g}{l}$	2 days	2.25 m H_2O	0.8 l	0.5 $\frac{g}{l}$	7.5 mg

The experiments were performed, and are plotted on **Figure 4.15**.

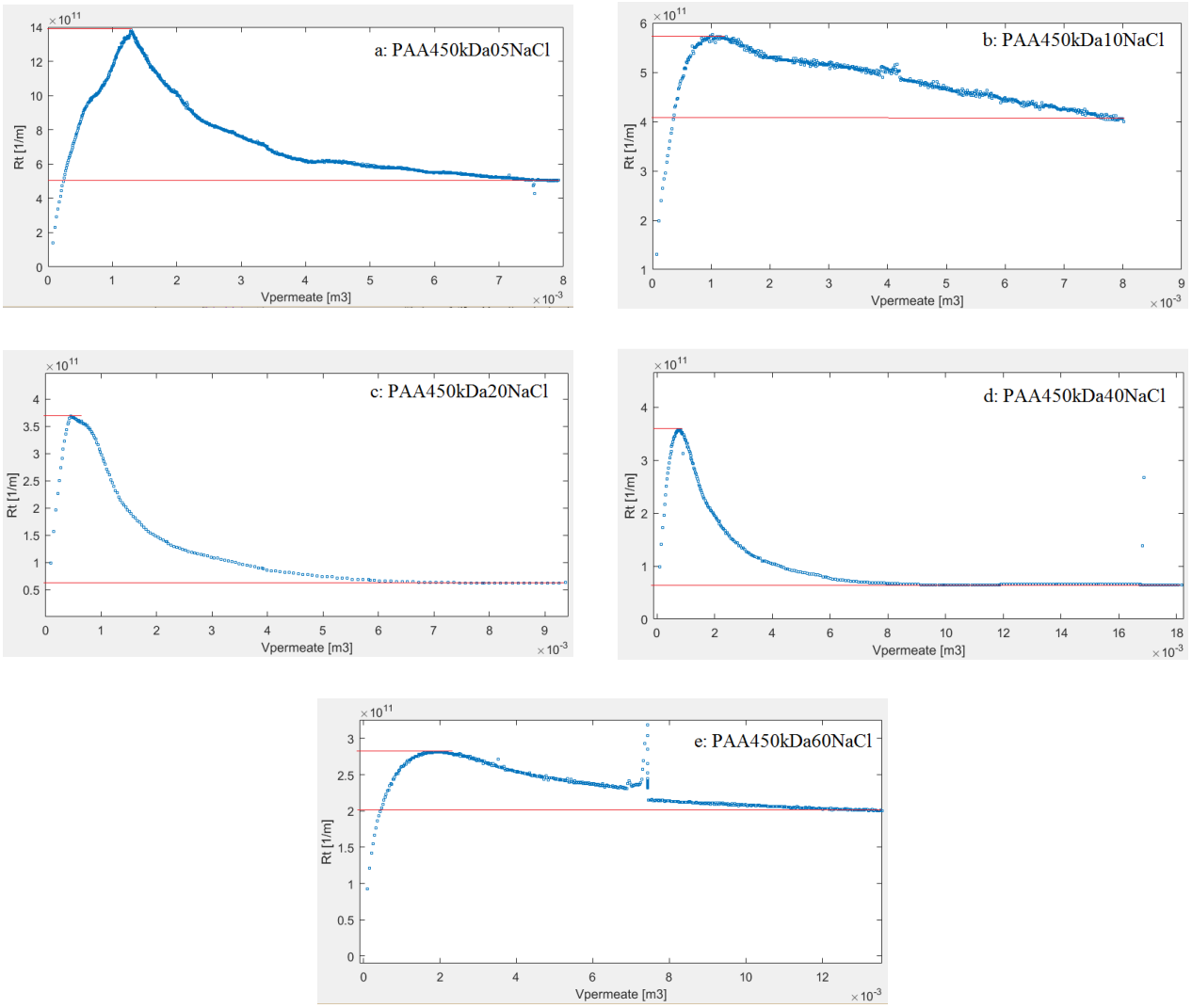

Figure 4.15: Here the data from the experiments in **Table 4.1** are plotted as the R_t^{app} as a function of the permeate volume. The horizontal red lines indicate the 'peak' and 'plateau' R_t^{app} listed in **Table 4.2** and plotted in **Figure 4.16**. **Figure a** is PAA450kDa05NaCl, **Figure b** is PAA450kDa10NaCl, **Figure c** is PAA450kDa20NaCl, **Figure d** is PAA450kDa40NaCl and **Figure e** is PAA450kDa60NaCl

Looking at the data, the results varies widely for each applied NaCl concentration. Generally, the tendency is similar to what has been previously observed: R_t^{app} increases as PAA450kDa is deposited, reaches a high point and then generally begins to fall towards a plateau in the R_t^{app}.

Table 4.2: Some of the data extracted from **Figure 4.15**. Peak location is how much permeate was produced when the peak in R_t^{app} is reached. Peak R_t^{app} is the peak resistance, and Plateau R_t^{app} is the approximate steady-state R_t^{app}.

NaCl	Peak location $[l]$	Peak R_t^{app} $[m^{-1}]$	Plateau R_t^{app} $[m^{-1}]$
0.5	1.3	14.0	5.0
1.0	1.1	5.7	4.1
2.0	0.7	3.7	0.6
4.0	0.9	3.8	0.6
6.0	2.0	2.8	2

The peak R_t^{app} is reached somewhere between 0.7 and 2.0 liters of permeate in all experiments. This is a bit inconsistent, but the range seems plausible, considering the PAA was dispersed in 0.8 l in the prechamber. The plateau R_t^{app} does not quite follow the trend observed in **Figure 4.4**, as seen on **Figure 4.16**.

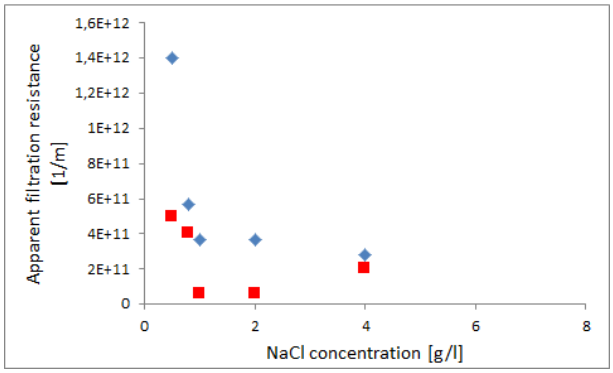

Figure 4.16: *Here the 'peak' and 'plateau' R_t^{app} is plotted as a function of the NaCl concentration of the feed, as the blue diamonds and the red squares, respectively.*

Nonetheless, a similar tendency of decreasing R_t^{app} with increased NaCl concentration is observed until approximately 2-4 $\frac{g}{l}$.

Because of the rather inconsistent data for the plateau-R_t^{app}, and the fact that experiments performed at higher pH caused the PAA R_t^{app} to not drop towards a plateau-R_t^{app}, possible leakage of PAA was investigated.

4.2.4 Investigating possible PAA450kDa leakage

The PAA450kDa polymer has a viscosity average molecular weight of 450 000 Da. With the monomer having a molecular weight of 72 Da, the polymer consists of around 6250 repeating units. As the polymer backbone consist merely of c-c bonds, we may estimate the total length of the polymer using the typical c-c bond length of 154 pm [Pauling and Brockway 1937]. The total stretched length of the polymer will be limited by the sp3 hybridization of the atoms in the polymer backbone. Each c-c bond in the backbone will then contribute with $l_{backbone,n_{unit}} = sin(\theta^\circ) * l_{c-c}$, where l is the respective length, and θ is half the angle between two bonds in sp3 hybridized molecules, 54°. The amount of c-c bonds n_{bonds} in the polymer depends on the repeating unit count (n_{unit}) through the relation $n_{bonds} = 1 + (n_{unit} - 1) * 2$.
Using this, we find that a single PAA of 450kDa should have a fully extended length of 1.56 μm. This matches the findings of Adamczyk et al. [2006], who conclude the length of PAA with a size of 12kDa to be 40.9 nm, which scaled to 450kDa results in an extended length of 1.52 μm.
As the membrane pore size is 0.22 μm, and the average hydrated diameter most likely significantly less than the fully streched length, PAA450kDa probably lies in a size range that may leak through the membrane.

To attempt to examine if PAA leakage might be the cause of the decrease in R_t^{app} towards a "plateau", an attempt to quantify the PAA on the membranes by titration was performed.

Examining PAA by titration

The methodology for performing the titrations included lowered the pH of the sample to 2.5 by addition of HCl, and then titrate the sample by a 0.005 M NaOH solution.
Titration of a prepared solution containing 20 mg PAA clearly allowed for determination of the presence of titratable groups, **Figure 4.17**.

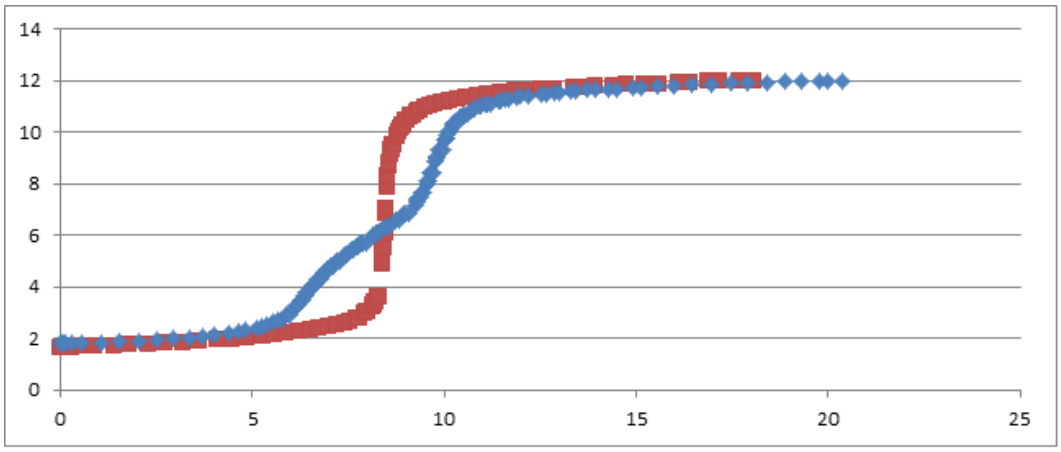

Figure 4.17: *The titration curves for an null sample (red line) and for a solution containing 20 mg PAA450kDa (blue line)*

By producing a plot of $\frac{\Delta pH}{\Delta V}$ as a function of volume of titrant used, **Figure 4.18**, we determine that 3.45 ml titrant has been used to neutralize the sample, meaning the sample contains 0.173 $mmol$ titratable groups. Considering the sample contained 20 mg PAA450kDa, with a monomer weight of 72 $\frac{g}{mol}$ and containing a single carboxylic acid per monomer, the expected amount of titratable groups is 0.278 $mmol$. This is a rather large difference, with only 62 % of the intended amount of PAA450kDa being detectable. A plausible explanation might be that the hygroscopic nature of PAA might have caused the PAA powder to absorb water, causing the weight measurement to overestimate the actual PAA450kDa content.
Examining a plot of $\frac{\Delta V}{\Delta pH}(pH)$, **Figure 4.19**, reveals that the PAA450kDa has a rather large spread of pKa values. Due to the polymeric nature of the compound, it is sensible that two neighbouring carboxylic acid groups are present in slightly different chemical environments, leading to difference in their association energy to protons, e.g. their pKa. Generally the pKa value appears to be between 6 $\pm$ 1, **Figure 4.19**, which is in accordance with litterature, in which pKa for PAA has been found to lie between 4.5 to 6.5 [Adamczyk et al. 2006, Pokhrel et al. 2000, Choi et al. 2005].

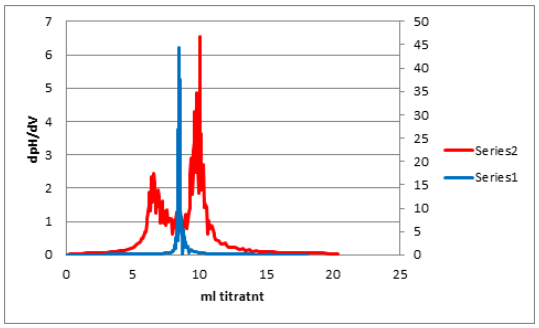

Figure 4.18: $\frac{\Delta pH}{\Delta V}$ *as a function of the volume of titrant for a solution of 20 mg PAA450kDa (red line) and for a null sample (blue line).*

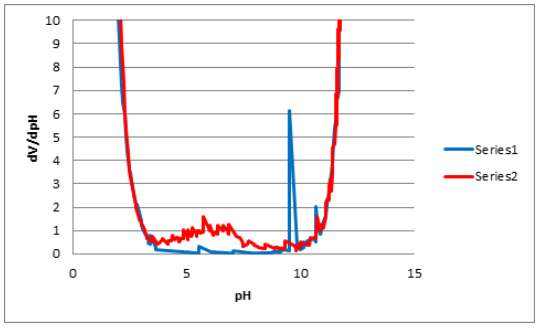

Figure 4.19: $\frac{\Delta V}{\Delta pH}$ *as a function of the pH for a solution of 20 mg PAA450kDa (red line) and for a null sample (blue line).*

Examining PAA content on membrane

In order to titrate the PAA on the membrane, the membrane were removed from the system after experiment PAA450kDa20NaCl, then folded and placed in plastic container. At a later point, the membrane was cut into pieces (**Figure 4.20**), and dispersed in 20 ml of 0.5 $\frac{g}{l}$ NaCl solution, and titrated similarly to before.

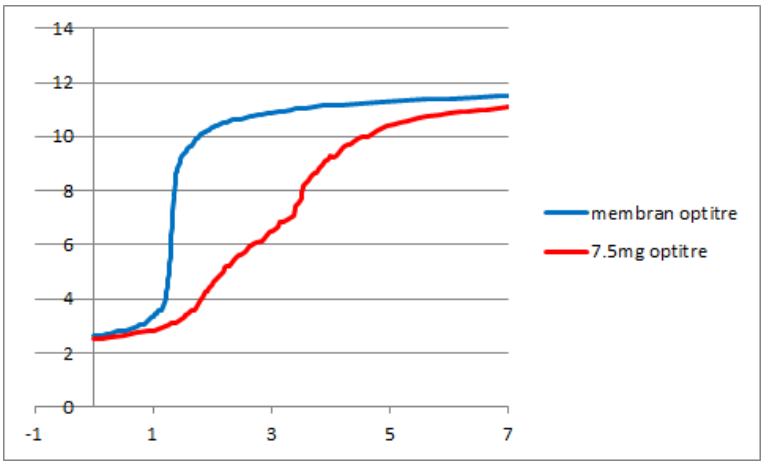

Figure 4.20: *Titration curves for a solution of 7.5 mg PAA450kDa (red line) and for a membrane on which 7.5 mg PAA450kDa should be deposited (blue line).*

The membrane titrated was used in experiment PAA450kDa20NaCl, in which 7.5 mg PAA450kDa was used. As a control sample, a solution containing 7.5 mg PAA was also titrated, see **Figure 4.20**.

The 7.5 mg PAA450kDa sample of **Figure 4.20** appear similar to the 20 mg PAA450kDa sample of **Figure 4.17**, clearly illustrating that this smaller amount of PAA450kDa is also detectable. If we examine the plot of $\frac{\Delta V}{\Delta pH}(pH)$ on **Figure 4.22**, a similar range of pKa values is also observed, albeit with more noise on the data.

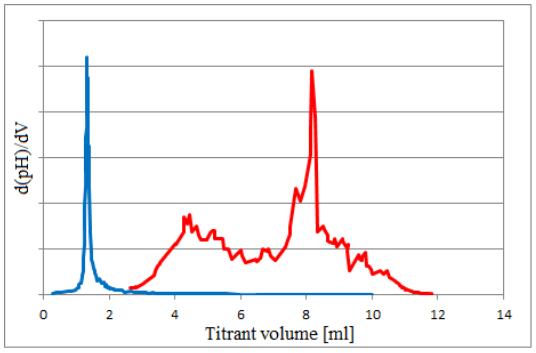

Figure 4.21: $\frac{\Delta pH}{\Delta V}$ *as a function of the volume of titrant for a solution of 7.5 mg PAA450kDa (red line) and for a membrane on which 7.5 mg PAA450kDa should be deposited (blue line).*

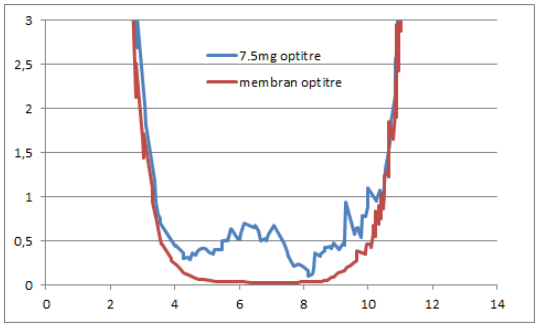

Figure 4.22: $\frac{\Delta V}{\Delta pH}$ *as a function of the pH for a solution of 7.5 mg PAA450kDa (blue line) and for a membrane on which 7.5 mg PAA450kDa should be deposited (red line).*

Examining **Figure 4.21**, 1.58 *ml* titrant was used in reaction with the sample, meaning 0.079 *mmol* of titratable groups were present. Of the expected 0.104 *mmol* PAA450kDa monomer, this means just 75 % of the intended PAA450kDa was detected, similar to the results of 62 % found in **Figure 4.18**.

However, when examining the titration of the sample with the membrane that should contain approximately 7.5 *mg* PAA45kDa, no detectable amount of PAA450kDa can be observed. Because of this indication that PAA450kDa might be leaking through the membrane, PAA with a molecular weight of 3000kDa (PAA3MDa) was acquired.

Filtration experiments with PAA3MDa was performed with just 1 *mg*, and the membranes from experiments PAA3MDa05NaCl and PAA3MDa10NaCl were titrated. Samples were prepared with 1 *mg* of PAA3MDa, to determine if this smaller amount of PAA could be detected. An example of a titration of 1 *mg* of PAA3MDa is found in **Figure 4.23** and the titration of the membrane from experiment PAA3MDa10NaCl is found in **Figure 4.24**.

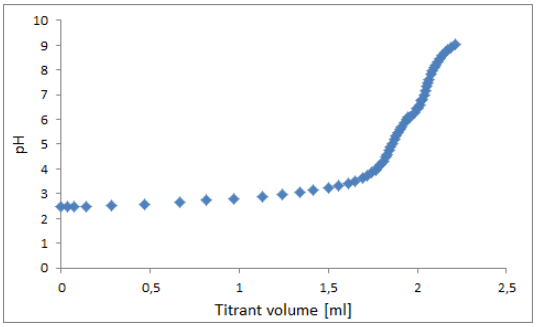

Figure 4.23: *The titration curve for a sample prepared with 1 mg of PAA3MDa. The presence of PAA3MDa can just barely be seen in the figure.*

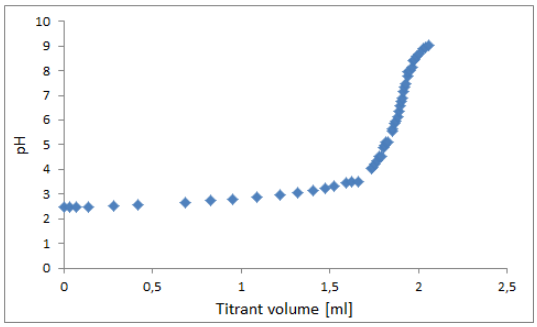

Figure 4.24: *The titration curve for a membrane on which 1 mg of PAA3MDa should be present. In the filtration curve, no presence of PAA can be determined.*

On **Figure 4.23**, the prepared sample containing 1 *mg* of PAA3MDa appears as a just barely detectable infliction point, and the content of the sample appears to be close to the detection limit of the titration setup used.
Similarly to the titration performed on the membranes with PAA450kDa, no apparent infliction point for carboxylic acid groups could be detected when a membrane was titrated, see **Figure**

4.24. The titration experiments therefore yielded inconclusive results about the presence of PAA on the membranes.

This may be caused by several factors. For one, when removing the membranes from the system, some liquid flushes across the membranes, which might wash off some PAA. Another cause might be that since the PAA is expected to be compressed onto the membrane, it might not readily re-dissolve into liquid and/or water diffusivity into the gel might be significantly hindered (as evident by the high R_t^{app}).

In conclusion, the titration experiments were unable to detect any PAA on any membranes used, but filtration experiments do clearly indicate that some PAA is deposited.

Either way, PAA3MDa was obtained, and further experiments were performed on this polymer.

Chapter 5 Results and discussion

5.1 Varying the amount of PAA3MDa

For the experiments, the continuous setup described in **Section 4.2.1** was used for filtrating water through PAA3MDa deposited on a 0.22 m pore size membrane. The membrane filtration resistance R_m was determined to be $1.5{*}10^{1}0\ m^{-1}$.

These experiments served two purposes: determining an amount of PAA3MDa suitable for experimenting with varying NaCl concentrations, and for examining how the mass of PAA3MDa on the membranes affect the filtration resistance. The experiments performed were performed with filtration parameters described in **Table 5.1**.

Table 5.1: A list of the experiments performed with varying amount of PAA3MDa. $[NaCl]_{feed}$ is the feed concentration of NaCl, t is the elapsed time of the experiment, ΔP is the filtration pressure, V_{dose} is the prechamber volume of PAA3MDa solution used, $[\mathrm{NaCl}]_{dose}$ is the NaCl concentration in the prechamber volume solution, m_{dose}^{PAA} is the mass of PAA3MDa dissolved in the dosage solution in the prechamber and ω is the expected mass of filter cake (PAA3MDa) per unit area.

Experiment ID	$[NaCl]_{feed}$	t	ΔP [kPa]	V_{dose}	$[\mathrm{NaCl}]_{dose}$	m_{dose}^{PAA}	$\omega\ [\frac{kg}{m^2}]$
PAA3MDa001mg	0.5 $\frac{g}{l}$	1.4 days	22	0.3 l	0.5 $\frac{g}{l}$	0.1 mg	$0.07{*}10^{-4}$
PAA3MDa005mg	0.5 $\frac{g}{l}$	1.2 days	22	0.3 l	0.5 $\frac{g}{l}$	0.5 mg	$0.36{*}10^{-4}$
PAA3MDa010mg	0.5 $\frac{g}{l}$	4.6 days	22	0.3 l	0.5 $\frac{g}{l}$	1.0 mg	$0.72{*}10^{-4}$
PAA3MDa015mg	0.5 $\frac{g}{l}$	3.9 days	22	0.3 l	0.5 $\frac{g}{l}$	1.5 mg	$1.08{*}10^{-4}$
PAA3MDa020mg	0.5 $\frac{g}{l}$	5.8 days	22	0.3 l	0.5 $\frac{g}{l}$	2.0 mg	$1.44{*}10^{-4}$
PAA3MDa075mg	0.5 $\frac{g}{l}$	1.4 days	22	0.3 l	0.5 $\frac{g}{l}$	7.5 mg	$5.41{*}10^{-4}$

The experiments were performed, which provided the following data, where R_t^{app} is plotted as a function of permeate volume, **Figure 5.1**.

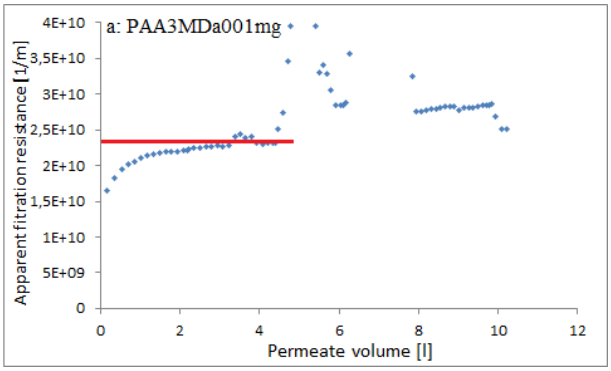

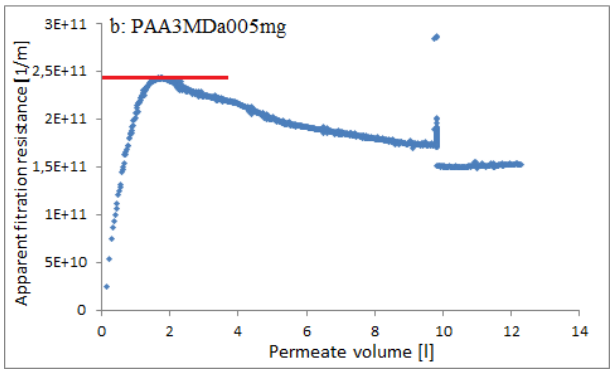

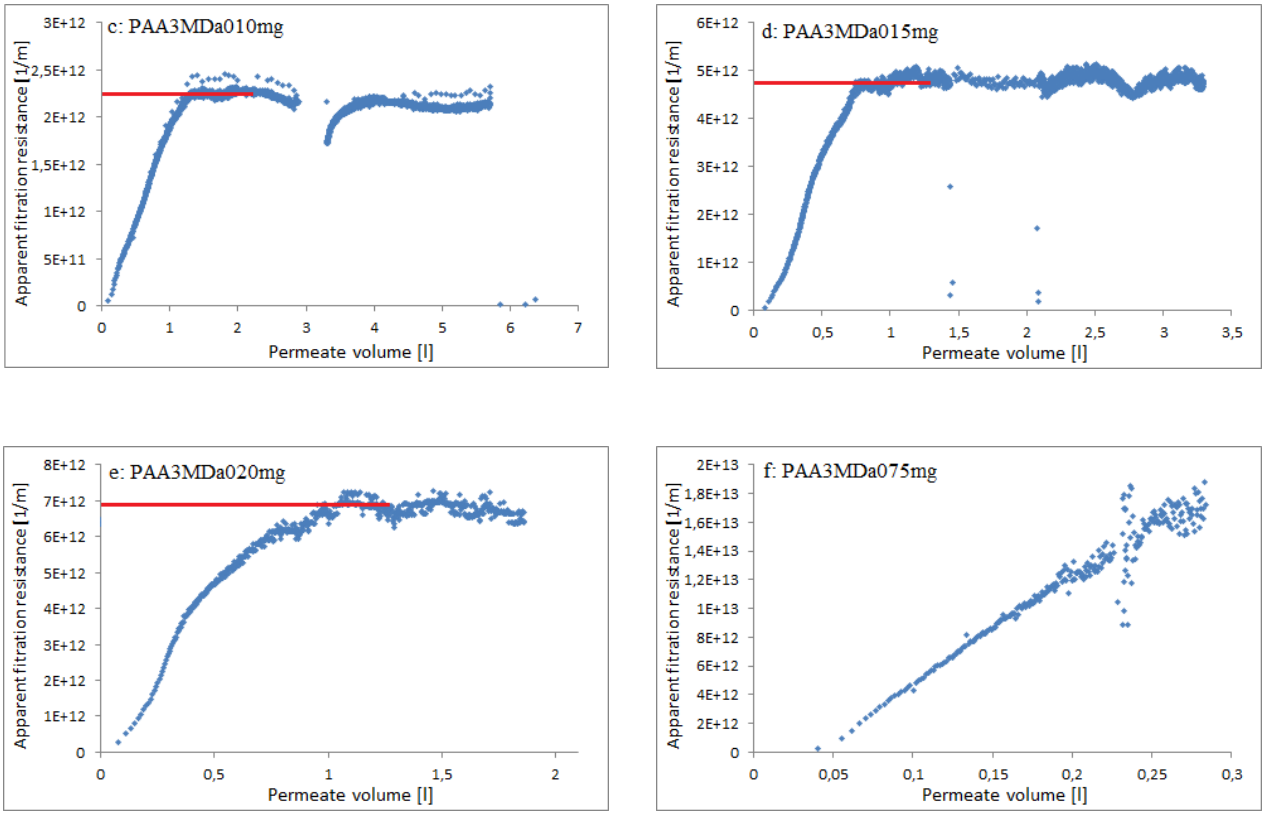

Figure 5.1: The experiments from **Table 5.1**, plotted as R_t^{app} as a function of the permeate volume. The red lines indicate the R_t^{app} used in **Figure 5.2**. **Figure a** is PAA3MDa001mg, **Figure b** is PAA3MDa005mg, **Figure c** is PAA3MDa010mg, **Figure d** is PAA3MDa015mg, **Figure e** is PAA3MDa020mg and **Figure f** is PAA3MDa075mg

Generally the R_t^{app} behaves quite differently than observed in **Section 4.2.3** when using PAA450kDa. For both polymers, a steep increase in R_t^{app} occurs as the PAA is deposited. However, this point is followed by a decrease in R_t^{app} for PAA450kDa, while for PAA3MDa, the R_t^{app} remains high, with the exception of PAA3MDa005mg. This could indicate that it probably is leakage of the PAA450kDa through the membrane that caused the R_t^{app} to drop over time, as observed in **Section 4.2**.

Examining when the R_t^{app} reach their maximum in these experiments, it is well before 2 l of permeate is produced in all of them, and is generally after about 1 l. As the prechamber volume is 0.3 l, this is a clear indication that the flow through the prechamber is not laminar, and some mixing occur between the dosage solution and the feed solution.
If we note the maximum R_t^{app} observed for each polymer concentration, we naturally see that the R_t^{app} increases as PAA3MDa mass is increased, **Figure 5.2**.

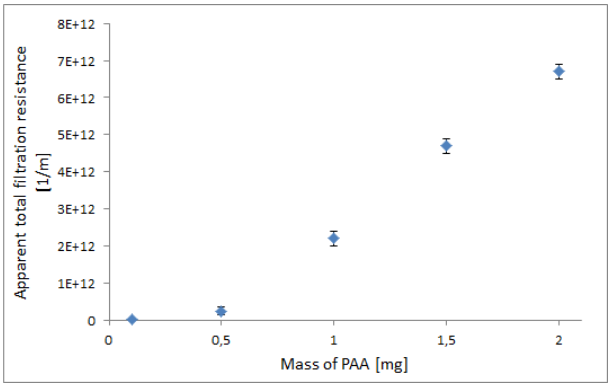

Figure 5.2: *The blue diamonds are the R_t^{app} as a function of the mass of PAA3MDa deposited on the membrane. The red line illustrates how a cake filtration with an α of $6{*}10^{15}\frac{m}{kg}$ would behave, if no other effects were influential*

Two features of **Figure 5.2** are especially striking: the apparently linear region of the dataset, and the offset from origin for this linear region.

If PAA3MDa would behave in a simple manner with an α of $6{*}10^{15}\frac{m}{kg}$, with no other effects influencing, the data is expected to appear as a linear relation which hits origin, see **Figure 5.2**. This model appear very similar to the observed data, with the exception that a linear regression of the observed data does not intercept in origin.

A plausible cause of this deviation from the simple model might be found in adsorption of PAA3MDa onto surfaces of containers during handling of PAA3MDa solutions. Adsorption of polyelectrolytes onto surfaces has been suggested in literature to be influential when dealing with low concentrations of polyelectrolytes ([Adamczyk et al. 2006]), and could be a systematic error for these measurements, which would explain the offset from origin. While plausible, this explanation does not appear completely convincing.

Another plausible cause for the data of **Figure 5.2** would be compressive effects happening on the PAA3MDa filter cake. At 0.1 *mg* of PAA, the membrane resistance contributes to about 60 % of the R_t^{app}, **Figure 5.3**. This means that during the first datapoints of the experiment series, the pressure drop across the filter cake layer is significantly less than the total filtration pressure, **Figure 5.4**. This means that the PAA3MDa experiences less compression in these datapoints, which could result in a lower specific filtration resistance of the filter cake.

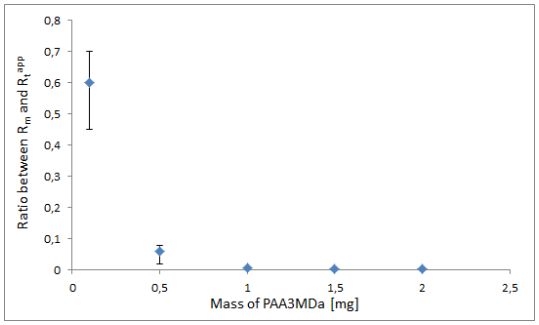

Figure 5.3: *The ratio of R_m to the R_t^{app} observed, as a function of the mass of PAA3MDa deposited on the membrane.*

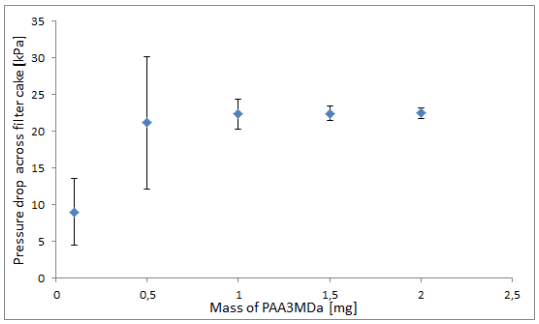

Figure 5.4: *The pressure drop across the filter cake, plotted over the mass of PAA3MDA deposited on the filter cake.*

In order to examine if the data may be explained by compressibility of the filter cake layer, an empirical expression which has previously been applied to examine compressive effects **Equation 5.1**, is applied [Tiller and Horng 1983] :

$$\alpha = \alpha_0 * (1 + \frac{P_s}{P_a})^{\eta} \qquad \textbf{(Equation 5.1)}$$

Where P_a is an empirical constant in given in pressure, α_0 is the specific flow resistance in an unstressed filter bed, β is a compressibility coefficient, and P_s is the pressure drop across the filter cake. A fit to the experimental data for specific filtration resistance and filter cake pressure, was completed with this model, **Figure 5.5**.

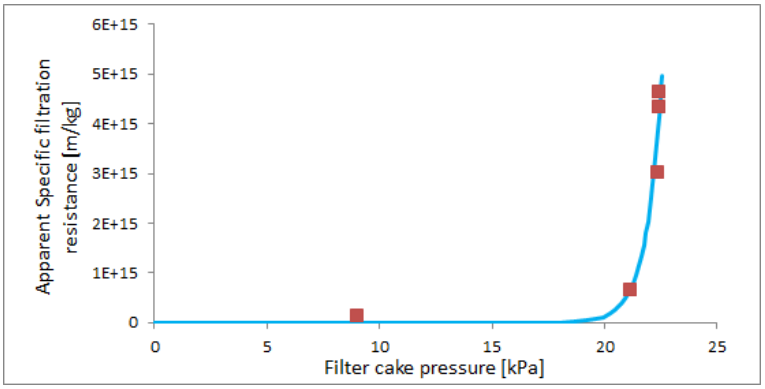

Figure 5.5: *The red squares are the specific filtration resistance α from the data of **Figure 5.2**, plotted as a function of the filter cake pressure P_s. The blue line is **Equation 5.1** fitted to the data by α_0 of 3.27 $\frac{m}{kg}$, P_a of 116736 Pa and η being 197.86*

The fit of the empirical expression can be fitted to the data, but not exceptionally well, with α_0 being 3.27 $\frac{m}{kg}$, P_a being 116736 Pa and η being 197.86.

However the constants obtained for this fit seem quite unrealistic, when compared to the range that they are typically observed to reside in. Tiller and Horng [1983] consider compressibility coefficients in the range of 0.2 to 1.5, in which they consider 0.2 to be describing a slightly compressible cake, while 1.5 is considered to describe an extremely compressive cake. A compressibility coefficient of 197.86 thus seem highly unlikely to be true. Therefore the dataset cannot be explained by compressive effects.

Another plausible cause for the offset observed in the dataset of **Figure 5.2** might be due to effects that occur in the first layer of filter cake. Effects such as pore-blocking and surface adsorption, would result in a linear region that extrapolates to be offset from origin, see **Figure 5.6** [Iritani et al. 2015].

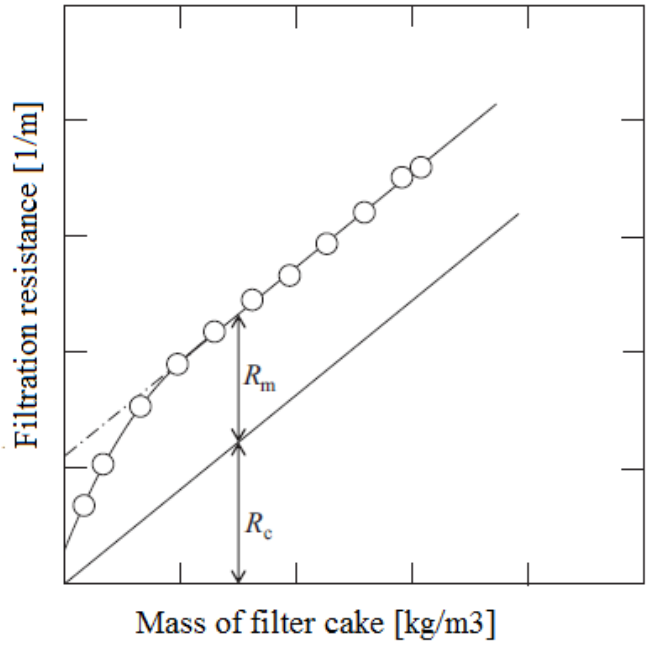

Figure 5.6: *A typical relation between filtration resistance and mass of cake deposited. The relation is mainly linear, but extrapolates to an offset from origin, caused by the membrane filtration resistance, and interfacial effects such as poreblocking. Figure from Iritani et al. [2015]*

While most interactions between the membrane surface and the first layers of filter cake, provide an increase in filtration resistance, other effects may provide a lower filtration resistance.

The membrane is made of polyethersulfone, which is a hydrophilic thermoplastic, see **Figure 5.7**.

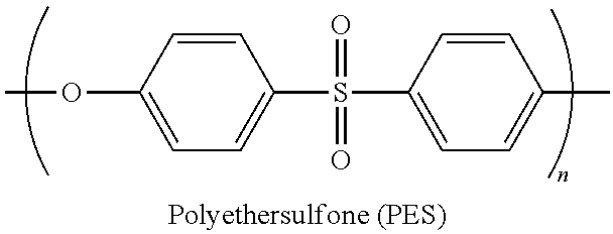

Figure 5.7: *Polyethersulfone, which is the material that the membrane consist of. Interactions between PAA3MDa and polyethersulfone could cause a different specific filtration resistance for the first layer of PAA3MDa.*

Interactions between PAA3MDa and the membrane surface could result in an offset from origin that extrapolates to a negative filtration pressure, as seen in **Figure 5.2**.

The cause for the offset may also be found in some PAA3MDa leaking through the membrane, before a proper cake layer is formed. The PAA450kDa with a lower molecular weight was found to leak through the membrane quite significantly, and some leakage through the membrane may also occur with PAA3MDa. The dataset of **Figure 5.2** could be explained by a small amount of PAA3MDa leaks through the membrane in each experiment.

Issues with the experimental method may also have an effect in this dataset. As confirmed before, the prechamber applied does not have a linear flow, and some mixing does appear to occur. This could result in an uneven distribution of PAA3MDa upon the membrane.

If we consider the PAA3MDa to have porosity of 0.86 [Jackson and James 1986] and a solid density of 1.43 $\frac{g}{cm^3}$ [Weiss and Silberberg], which are data for a polyacrylamide gel, a polymer structurally similar to PAA, we may estimate an approximate thickness of the filter cake. Using these values, 0.1 mg of PAA3MDa on the membrane would only create a cake layer of 36 μm thickness. It does not appear inconceivable that this layer might be unevenly distributed on the membrane, especially considering the apparent mixing taking place in the prechamber.

An uneven distribution of polymer on the membrane could lead to 'shortcuts', causing a systematically lower R_t^{app}.

In conclusion, the linear nature of the majority of the dataset does indicate that the R_t^{app} does mostly act like a normal cake deposition when additional PAA3MDa is added. The offset off of origin cannot be explained by compressive effects. Potentially systematic errors during experiment preparation could explain the offset, and the errors could be adsorption of PAA3MDa to surfaces and/or uneven filter cake layer due to mixing in the prechamber. However systematic errors seem quite unlikely, as some variation should be expected for the proposed plausible causes for the error. Instead, the cause may lie in either leakage of PAA3MDa through the membrane, or certain effects taking place in the first filter cake layer, due to interactions with the membrane surface.

Regarding a suitable mass of PAA3MDa to use for further experiments, 1 mg was chosen due to being in the linear region of **Figure 5.2**, while still resulting in a flow high enough for making experiments last about 2 days or less.

5.2 Influence of NaCl upon the apparent filtration resistance

Using 1 mg of PAA3MDa, experiments similar to those explained in **Section 5.1** were performed with variations in the NaCl concentration in the feed water.
About a day into each experiment, the filtration pressure was changed from 22 kPa to 7.4 kPa, and 12 hours after changed back to 22 kPa.
The following experiments were performed:

Table 5.2: A list of the experiments performed with varying concentration of NaCl in feed. $[NaCl]_{feed}$ is the feed concentration of NaCl, t is the elapsed time of the experiment, ΔP is the filtration pressure, V_{dose} is the prechamber volume of PAA3MDa solution used, $[\text{NaCl}]_{dose}$ is the NaCl concentration in the prechamber volume solution, m_{dose}^{PAA} is the mass of PAA3MDa dissolved in the dosage solution in the prechamber and ω is the expected mass of filter cake (PAA3MDa) per unit area.

Experiment ID	$[NaCl]_{feed}$	t	ΔP [kPa]	V_{dose}	$[\text{NaCl}]_{dose}$	m_{dose}^{PAA}	ω $[\frac{kg}{m^2}]$
PAA3MDa02NaCl	0.2 $\frac{g}{l}$	2.9 days	22	0.3 l	0.5 $\frac{g}{l}$	1.0 mg	$0.72{*}10^{-4}$
PAA3MDa05NaCl	0.5 $\frac{g}{l}$	4.6 days	22	0.3 l	0.5 $\frac{g}{l}$	1.0 mg	$0.72{*}10^{-4}$
PAA3MDa10NaCl	1.0 $\frac{g}{l}$	2.2 days	22	0.3 l	0.5 $\frac{g}{l}$	1.0 mg	$0.72{*}10^{-4}$
PAA3MDa20NaCl	2.0 $\frac{g}{l}$	1.8 days	22	0.3 l	0.5 $\frac{g}{l}$	1.0 mg	$0.72{*}10^{-4}$
PAA3MDa40NaCl	4.0 $\frac{g}{l}$	2.1 days	22	0.3 l	0.5 $\frac{g}{l}$	1.0 mg	$0.72{*}10^{-4}$
PAA3MDa60NaCl	6.0 $\frac{g}{l}$	2.2 days	22	0.3 l	0.5 $\frac{g}{l}$	1.0 mg	$0.72{*}10^{-4}$

The experiments were performed, which provided the following data, where the R_t^{app} is plotted as a function of permeate volume.

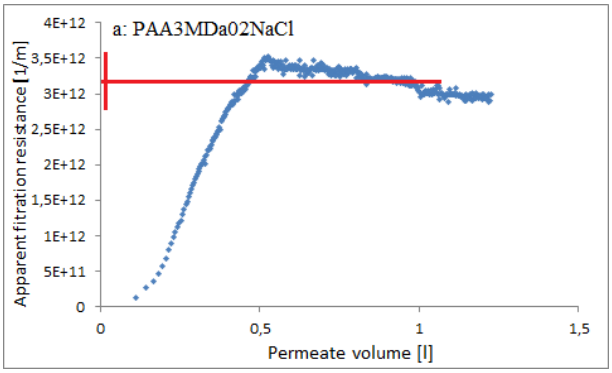

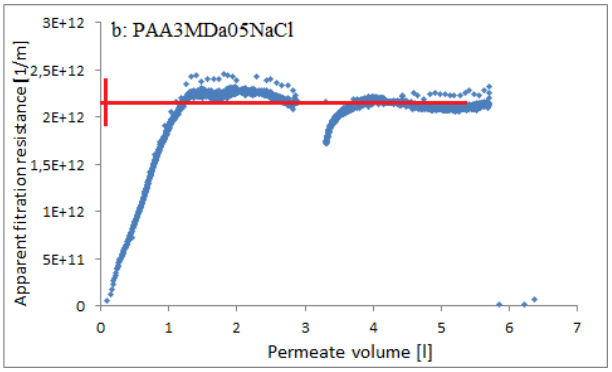

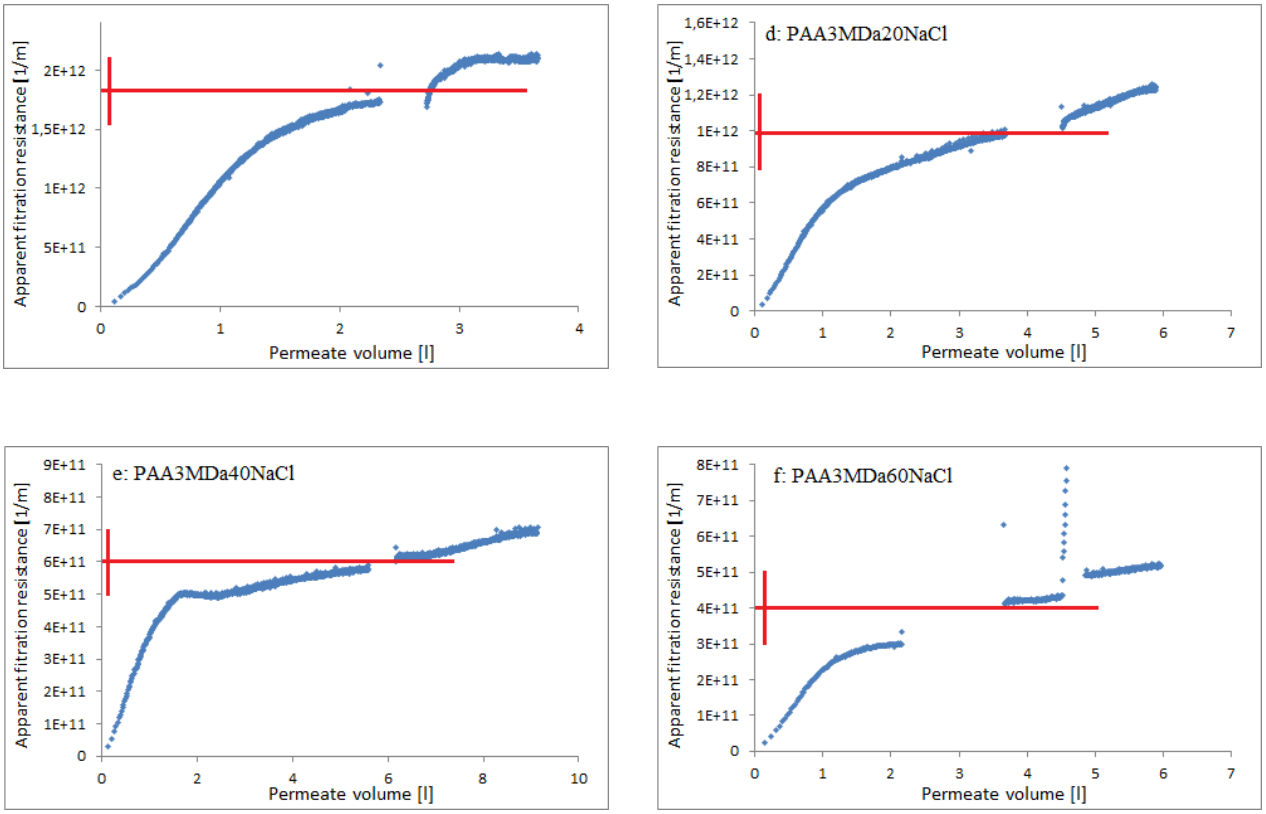

Figure 5.8: The experiments from **Table 5.2**, plotted as R_t^{app} as a function of the permeate volume. The red lines indicate the R_t^{app} used in **Figure 5.9**, with their respective inaccuracy of determination. **Figure a** is PAA3MDa02NaCl, **Figure b** is PAA3MDa05NaCl, **Figure c** is PAA3MDa10NaCl, **Figure d** is PAA3MDa20NaCl, **Figure e** is PAA3MDa40NaCl and **Figure f** is PAA3MDa60NaCl

Figure 5.8 visualizes some rather messy data, which occasionally are caused by some limitations of the setup used. However, the regions of the datasets are still usable.

As the filtration pressure is changed during the experiment, a region appears where no data is visible.

The lack of data in this region is caused by the filtration pressure being reduced to 7.4 kPa from 22 kPa, which the data treatment process has not accounted for. The consequences of the changes in filtration pressures will be dealt with in **Section 5.4**.

Generally though, the data looks as expected. Within approximately 2 l of permeate being produced, it appears most of the PAA3MDa has been deposited, as R_t^{app} does not appear to increase much further. In some of the datasets, the R_t^{app} does continue to increase slightly during filtration after the first 2 l permeate has been produced, but the cause of this remains unexplained.

By noting the obtained R_t^{app} after the PAA3MDa was deposited, as observed on **Figure 5.8**, we plot it as a function of the NaCl concentration of the feed, **Figure 5.9**.

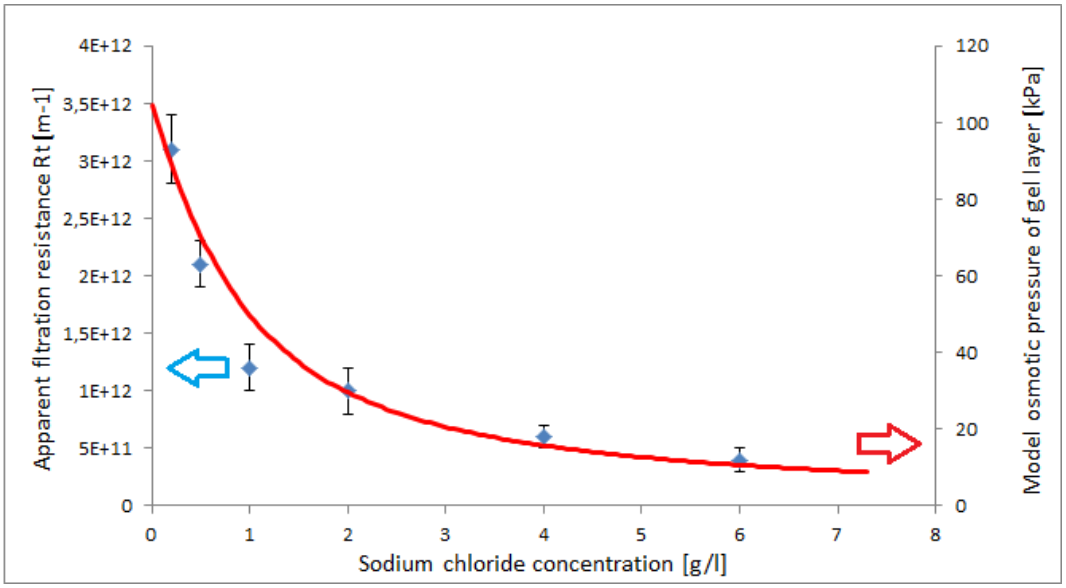

Figure 5.9: *The R_t^{app} of **Figure 5.8** is plotted as the blue diamonds, and is plotted with the model from **Section 2.5**, using a charge count consistent with 1 mg of PAA, dispersed in a gel volume corresponding to a cake layer thickness of 202 μm. The trends appear visually similar, but cannot be directly compared*

Examining how the R_t^{app} is affected by the NaCl concentration of the feed water, see **Figure 5.9**, we manage to get a quite clear relation. The general relation is similar to what was observed for the plateau R_t^{app} of PAA450kDa in the piston setup (**Figure 4.4**) and in the continuous setup (**Figure 4.16**), but is vastly more apparent.

If we use the model from **Section 2.5**, and consider 1 mg of PAA3MDa to be dispersed evenly in a volume of $0.28ml$, found by assuming the PAA density being 1.43 $\frac{g}{cm^3}$ ([Weiss and Silberberg] for PAM) and assuming a porosity of 0.997, resulting in a gel layer thickness of 202 μm, we acquire a relation between the NaCl concentration in bulk solution and the osmotic pressure of the gel volume, illustrated on **Figure 5.9**.

It clearly appears that the model and the experimental data follows a similar trend, though the data types cannot be directly compared. Furthermore, for this range of NaCl concentrations, the model predicts osmotic pressures ranging from 0.2 to 1.4 bar, while the actual experiments were run with 225 cmH_2O, equalling about 0.225 bar. Obviously, applying the osmotic pressures for estimating flux by using Darcy's law through standard methods therefore make no physical sense, as this would predict an inverted flux.

If we assume that the PAA3MDa filter cake has no filtration resistance and that only the membrane contributes to the filtration resistance of the system, ie. R_t=R_m, we may calculate which osmotic pressure would explain the data, π^{app}, see **Figure 5.10**.

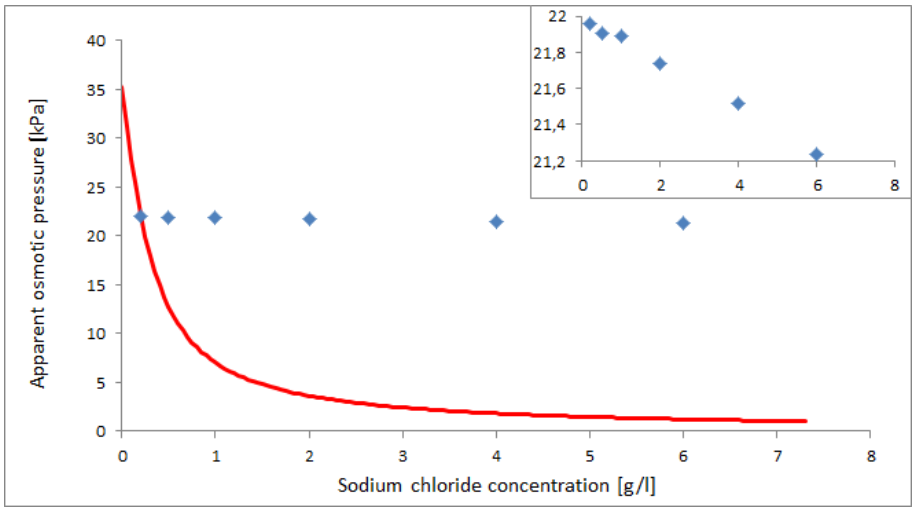

Figure 5.10: *The blue diamonds are π^{app}, which are found by assuming that only the membrane contributes to R_t, and calculating which value of π could explain the obtained flux, π^{app}. The red line is the model of* ***Section 2.5****, using the same parameters as in* ***Figure 5.9****, but assuming a larger cake thickness of 0.5 mm. The insert figure is an enlargened image of π^{app}.*

As evident in **Figure 5.10**, π^{app} changes very little with the NaCl concentration, and the model from **Section 2.5** is unable to match the trend observed.

In conclusion, R_t^{app} for a PAA filter cake decreases significantly and with a clear trend, as the NaCl concentration of the feed is increased. The trend is visually similar to a simple model of osmotic pressure of a polyanionic gel, based on Donnan-equilibria. If the PAA filter cake was assumed to exhibit no filtration resistance, π^{app} was found to decrease very little with NaCl addition, and did not follow the model of **Section 2.5**.

The increase in concentration of electrolytes may affect polyionic substances in many ways, including various electrostatic and hydrodynamic interactions, and could cause changes to the structure and volume of the PAA filter cake.

However it does not seem likely that the data of **Figure 5.9** can be explained only by changes in the volume and structure of the PAA filter cake, and the resulting changes to the hydraulic resistance to flow.

Regarding changes to the structure of the PAA filter cake, [Adamczyk et al. 2006] have found that the shape and effective length of PAA will be affected by the electrolyte concentration. Jackson and James [1986] examined how the orientation of fibers in a porous media affected the permeability. Within the category of randomly orientated 3d networks, the authors concluded that the permeability was only affected to a minor degree, by changes in the structure of these 3d networks. So changes in the structure of the PAA with increased NaCl concentration would probably not cause any significant changes to the permeability.

Regarding changes to the volume of the PAA filter cake, Yin et al. [2009] examined how a polyelectrolyte gel behaves when in contact with reservoir of monoelectrolytes, and found that an increase in monoelectrolytes causes a polyelectrolyte gel to deswell. Similarly, other authors have found that sludge deswells when it comes in contact with higher concentrations of NaCl, and concluded that this was also caused by the presence of polyelectrolytes [Curvers et al. 2009,

Lin et al. 2014a]. As the PAA filter cake examined in this study is polyelectrolytic in nature, we will expect that the PAA filter cake similarly will decrease in volume, at higher concentrations of monovalent electrolytes. As the filter cake deswells, the resulting decrease in porosity is expected to cause an increase in hydraulic filtration resistance [Jackson and James 1986]. This predicts an increase in hydraulic filtration resistance, with increased NaCl conctration, which is in contradiction to the actual relation observed in **Figure 5.9**.

The data in **Figure 5.9** therefore cannot be easily explained by the NaCl concentration causing changes to the structure and volume of the PAA filter cake. We have not been successful in explaining what causes the flux across a PAA filter cake to increase as NaCl concentration of the feed is increased. A calculated π^{app} for the experiments showed no similarity with the model for osmotic pressure in gel-like volume from **Section 2.5**. However, a visual similarity between the osmotic pressure model and experimental data for R_t^{app} is remarkable in **Figure 5.9**. Because R_t^{app} is influenced by changes in osmotic pressure, the visual relation on **Figure 5.9** was found to be an indication that osmotic pressure of the filter cake does influence the flux, and that the osmotic pressure of the filter cake is influenced by the NaCl concentration by Donnan-equilibria.

5.3 Compressibility of the cake layer

An experiment was performed where 1 mg PAA3MDa was deposited on a membrane, and then the filtration pressure was altered with intervals, for most intervals about 12 hours. The feed and prechamber solutions were both prepared with 0.5 $\frac{g}{l}$ NaCl. The prechamber volume was 300 ml.
The data is plotted in **Figure 5.11**.

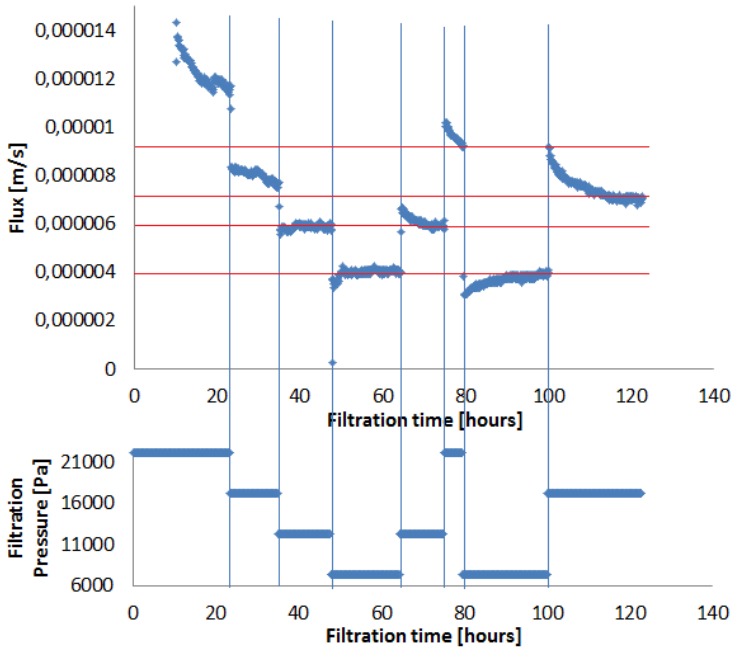

Figure 5.11: *On the upper figure, flux is plotted as a function of time. On the lower figure, the schedule for ΔP is illustrated. The vertical blue lines are guides to help distinguish between the different ΔP, and the horizontal red lines indicate the steady-state flux for each ΔP, that is used in* ***Figure 5.12****. The experiment was performed by depositing 1 mg of PAA3MDa on the membrane, and then changing the filtration pressure in intervals.*

As evident on **Figure 5.11**, when the filtration pressure is changed, some time passes before the flux reaches steady state at the new filtration pressure.

If we take a look at the steady state fluxes obtained for each filtration pressure, 7.4 and 12 kPa reach practically the same flux in their latter regions, as in their prior regions. 17 kPa reach nearly the same flux in both regions, but the flux is slightly higher the first time. The cause may simply be that the PAA3MDa was not fully deposited in the first one, which is indicated by the flux not reaching a steady state before the filtration pressure was changed. The regions where the filtration pressure was 22 kPa, the flux did not quite reach steady state in either region. The steady state flux for 22 kPa is noted to be $9.2{*}10^{-6}\frac{m}{s}$.
The steady state flux obtained for a given pressure, appear to be reaching the same flux, independent of the prior filtration pressures, see **Figure 5.11**. This indicates that only reversible changes to the filter cake are taking place following changes in filtration pressures, within the time frame of this experiment.

These steady state fluxes are all indicated on **Figure 5.11** by the red lines, converted to the α^{app} of the filter cake, and are plotted as a function of the pressure drop across the filter cake, **Figure 5.12**.

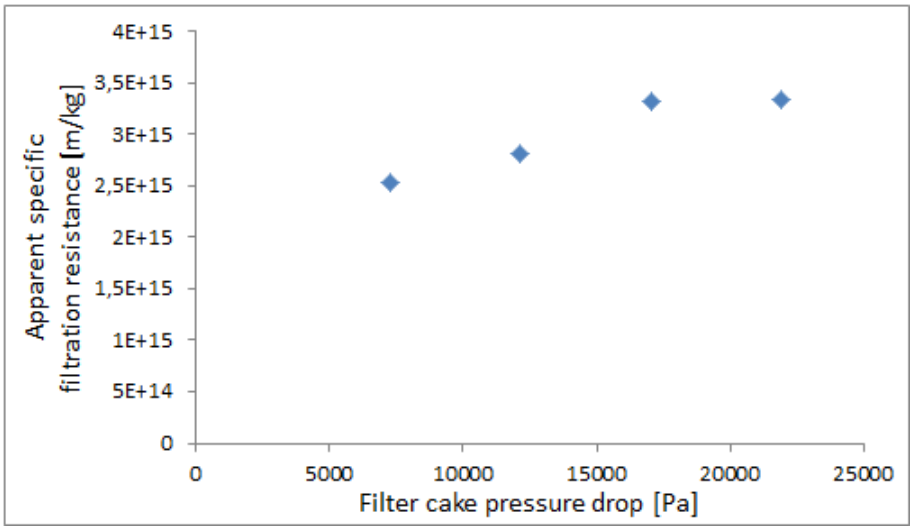

Figure 5.12: α^{app} *of the filter cake from* ***Figure 5.11****, plotted as a function of the filter cake pressure* P_s.

The empirical expression **Equation 5.1** was also fitted to this data, illustrated on **Figure 5.12**, which resulted in a compressibility factor η of 1.14, which lies within the range that Tiller and Horng [1983] refers to as a "very compressible" filter cake.

5.4 Influence of NaCl upon the compressibility of the cake layer

The same dataset of **Section 5.2** is now plotted as flux as a function of time.

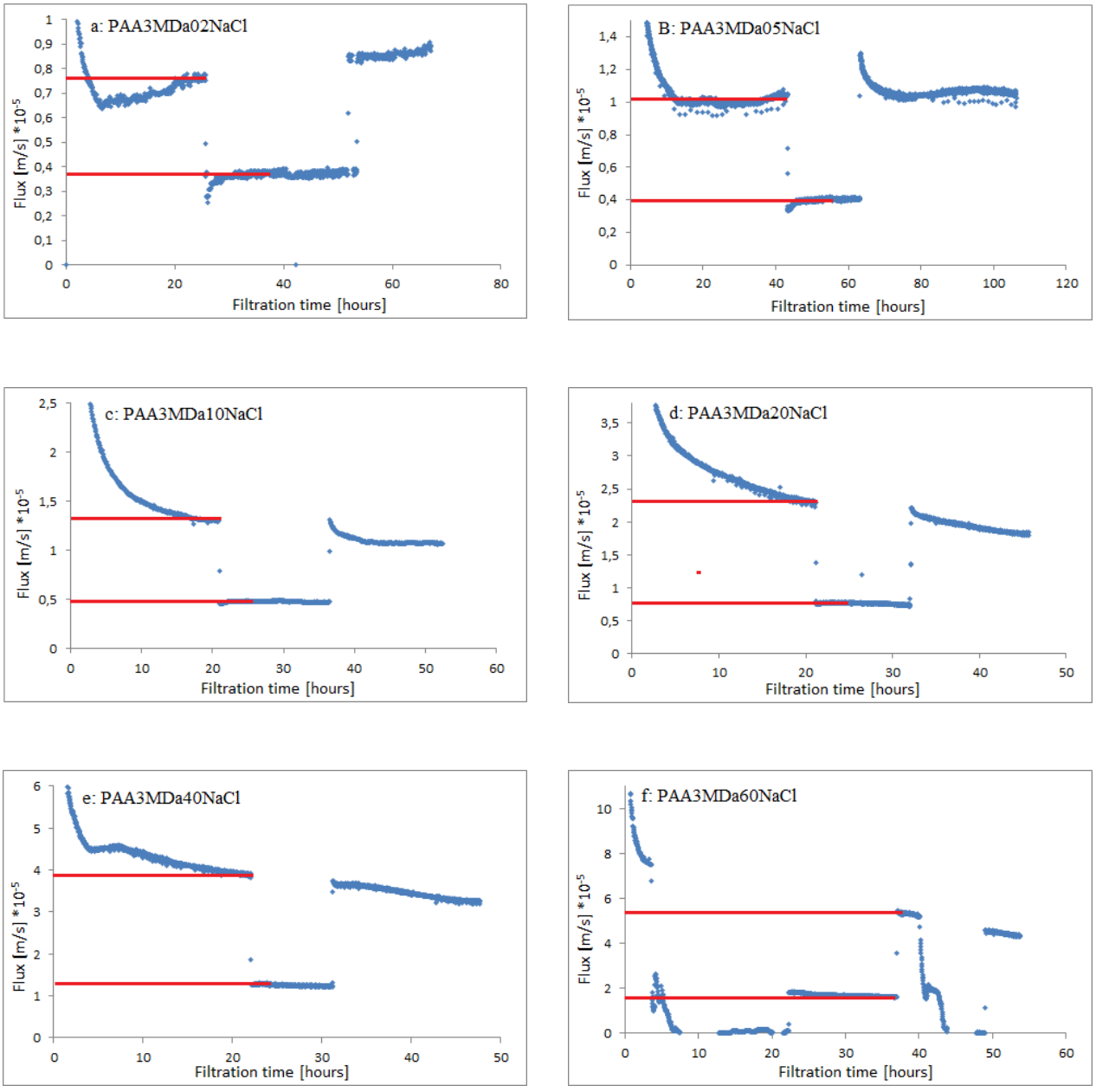

Figure 5.13: The experiments from **Table 5.2**, plotted as flux over the elapsed filtration time. The abrupt offset near the middle of each dataset is caused by the ΔP being changed from 22 kPa to 7.4 kPa and back again. The red lines indicate the fluxes for ΔP of 22 and 7.4 kPa used for making **Figure 5.9**. **Figure a** is PAA3MDa02NaCl, **Figure b** is PAA3MDa05NaCl, **Figure c** is PAA3MDa10NaCl, **Figure d** is PAA3MDa20NaCl, **Figure e** is PAA3MDa40NaCl and **Figure f** is PAA3MDa60NaCl

In the figures, the determined steady-state fluxes are indicated for both 22 and 7.4 kPa ΔP by the red lines. It can be observed that immediately after a change in filtration pressure, the

flux requires some time before it reaches steady state at a new pressure.

The steady-state fluxes obtained for each NaCl concentration, at filtration pressures of both 22 and 7.4 kPa, as indicated by the red lines on **Figure 5.13**, where converted to R_t^{app} and plotted as a function of the NaCl concentration, see **Figure 5.14**.

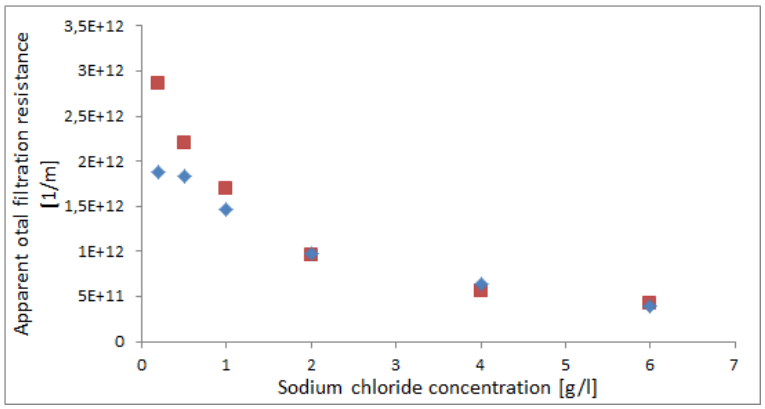

Figure 5.14: *The fluxes obtained for each NaCl concentration, at ΔP of both 22 and 7.4 kPa, was converted to R_t^{app} for the filter cake, and plotted as a function of the NaCl concentration in the feed water. The blue diamonds are the R_t^{app} obtained at a ΔP of 7.4 kPa, and the red squares are the R_t^{app} obtained at a ΔP of 22 kPa*

Increasing the ΔP causes a higher driving force for liquid to pass through the membrane and the filter cake. If the increase in ΔP causes filter cake on the membrane to compress, and reduce the volume it occupies, the filter cake will exert a higher filtration resistance due to the reduced porosity of the filter cake [Jackson and James 1986]. In the case of a polyanionic filter cake, the concentration of polyanions in the filtercake similarly increases, which according to the model in **Section 2.5** will cause the filter cake to exert a higher osmotic pressure. Both effects are expected to reduce the flux, and result in an increase in R_t^{app}.

Similarly, if an increase in ΔP does not cause any changes to the structure and porosity of a filter cake, neither the hydraulic filtration resistance, nor the osmotic pressure of the counterions are expected to change, and the R_t^{app} should not change.

By this reasoning, if we observe that the R_t^{app} increases as the ΔP is increased, we expect that it is caused by the filter cake being compressed, as that effect is expected to result in both a higher filtration resistance, but also in a higher osmotic pressure of the filter cake.

We take the data of **Figure 5.14**, and find the increase in R_t^{app} from a ΔP of 7.4 to 22 kPa, and plot it as a function of the NaCl concentration, **Figure 5.15**.

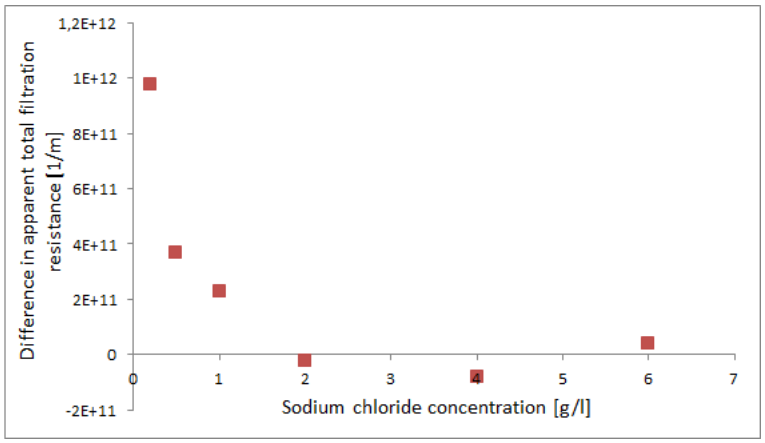

Figure 5.15: *The difference in R_t^{app} observed for a ΔP of 7.4 to 22 kPa, plotted as a function of the NaCl concentration.*

We observe in **Figure 5.15** that the R_t^{app} does increase with increase in filtration pressure, but only to a detectable degree for NaCl concentrations 0.2, 0.5 and 1.0 $\frac{g}{l}$. This indicates that when the NaCl concentration is low, the filter cake is able to be compressed by higher filtration pressures. As the change in aR_t^{app} appears reversible (see **Figure 5.13.b** as an example), some force must be counteracting the compression. Such an effect could be caused by structural effects such as elasticity of the filter cake, but osmotic pressure is an obvious candidate for causing the filter cake to swell.

For higher concentrations of NaCl, we observe little to no change in R_t^{app} in **Figure 5.15**, indicating that an increase in ΔP causes no significant structural change in the filter cake. This may be caused by several effects, but it may be explained by osmotic pressure as well. If the osmotic pressure of the filter cake is reduced at a higher NaCl concentration, as predicted in **Section 2.5**, the ability of the filter cake to swell should be reduced as well. A reduced ability to swell, may cause the filter cake to be compressed to a state where strong structural effects causes high resistance against further compression, and as such an increase in ΔP would not cause a significant change in filter cake porosity and thus in R_t^{app}.

A study by Lin et al. [2014a] used a sample of filter cake layer from an MBR, which contained EPS, with a water content of 37.58 %, and examined its water uptake when placed in solutions with various NaCl concentration, see **Figure 5.16**.

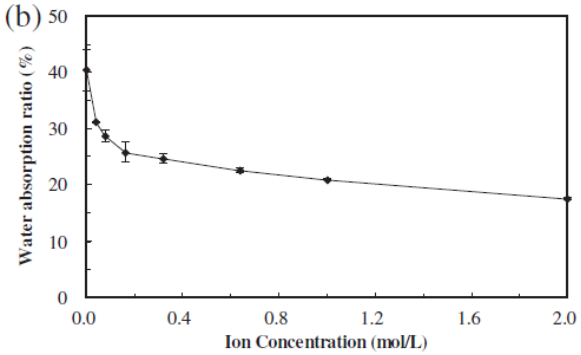

Figure 5.16: *Water uptake ratio found by immersing pieces of filter cake extracted from a lab-scale MBR in various NaCl solutions, figure taken from Lin et al. [2014a]*

Their data show that the filter cake deswells when in contact with solutions with a higher NaCl concentration. Curvers et al. [2009] similarly found that sewage sludge sediment volume reduced with increase in NaCl concentration. Both papers conclude that osmotic effects are causing this behaviour.

Their conclusions may be considered in relation to the discussion of the data in **Figure 5.15**. At low NaCl concentrations, osmotic pressure causes a polyanionic gel-like filter cake to swell [Curvers et al. 2009, Lin et al. 2014a]. As the ability of a substance to swell and to compress are closely related, it appears plausible that a reduction in the ability to swell, causes a reduced ability for reversible compression.

Chapter 6 Conclusion

An experimental setup was developed to test how polyacrylic acid behaves in filtration scenarios.

The apparent filtration resistance of a filter cake layer of polyacrylic acid was highly dependant upon the concentration of sodium chloride. Increasing the concentration of sodium chloride caused the apparent filtration resistance to decrease.

This could not be well explained by changes in hydraulic flow resistance, caused by sodium chloride causing structural changes to the filter cake. In literature, both polyelectrolyte gels and sludge containing polyelectrolytes has been documented to deswell with an increase in electrolyte concentration. The thereby reduced porosity of the PAA filter cake would result in an increase in hydraulic flow resistance. Instead, the apparent filtration resistance was observed to be reduced with an increase in sodium chloride concentration.

A simple model based on Donnan-equilibrium theory that estimates the osmotic pressure of a polyanionic gel in contact with a bulk solution of monovalent monoatomic ions was created. The model was unable to match the experimentally obtained apparent osmotic pressure, found by assuming that the filtration resistance consisted only of the membrane resistance. However, the model was applied on a system that corresponds to the parameters used in the experiments, and assuming a gel-layer volume of 0.28 ml, the observed relation between osmotic pressure and sodium chloride concentration is visually very similar to the trend observed for apparent filtration resistance. As the apparent filtration resistance will be affected by both the actual filtration resistance and the osmotic pressure, this was seen as an indication that the osmotic pressure of the filter cake does affect the flux, and that the osmotic pressure of the filter cake is influenced by the sodium chloride concentration through Donnan-equilibria.

Experiments found that polyacrylic acid behaves compressible when used as a filter cake during filtration. The compressibility of the filter cake was found to lower drastically with increased concentration of monovalent monoatomic ions, approaching an incompressible filter cake at high sodium chloride concentrations. This behaviour might be explained by the osmotic pressure of the filter cake being reduced with sodium chloride additions. A reduction of osmotic pressure of the polyanionic filter cake with addition of sodium chloride, would mean a lower tendency to swell, which matches findings in literature. A reduced ability to swell could plausibly cause a reduced ability for reversible compression.

In conclusion, in this project we observed several curious changes to the filtration characteristics of polyacrylic acid, that was being caused by the addition of sodium chloride. An approach that considered the osmotic pressure that arises in the polyacrylic acid filter cake was able to provide plausible explanations to as why the addition of sodium chloride would cause a reduction in apparent filtration resistance, and a reduction in the compressibility of the filter cake.

Bibliography

Adamczyk et al., **2006**. Z. Adamczyk, A. Bratek, B. Jachimska, T. Jasiski, and P. Warszyski. *Structure of Poly(acrylic acid) in Electrolyte Solutions Determined from Simulations and Viscosity Measurements.* The Journal of Physical Chemistry B, 110(45), 22426–22435, 2006. PMID: 17091984. 35, 36, 42, 49

Chang and Kaplan, **1977**. Raymond Chang and Lawrence J. Kaplan. *The Donnan equilibrium and osmotic pressure.* Journal of Chemical Education, 54(4), 218, 1977. 17, 18

Chen et al., **2012**. Jianrong Chen, Meijia Zhang, Aijun Wang, Hongjun Lin, Huachang Hong and Xiaofeng Lu. *Osmotic pressure effect on membrane fouling in a submerged anaerobic membrane bioreactor and its experimental verification.* Bioresource Technology, 125, 97 – 101, 2012. ISSN 0960-8524. 13, 15

Choi et al., **2005**. Jeeyoung Choi, and Michael F. Rubner. *Influence of the Degree of Ionization on Weak Polyelectrolyte Multilayer Assembly.* Macromolecules, 38(1), 116–124, 2005. 36

Curvers et al., **2009**. Daan Curvers, Shane P. Usher, Adam R. Kilcullen, Peter J. Scales, Hans Saveyn and Paul Van der Meeren. *The influence of ionic strength and osmotic pressure on the dewatering behaviour of sewage sludge.* Chemical Engineering Science, 64 (10), 2448 – 2454, 2009. ISSN 0009-2509. 13, 15, 49, 56

Curvers et al., **2011**. Daan Curvers, Hans Saveyn, Peter J. Scales and Paul Van der Meeren. *Compressibility of biotic sludges – An osmotic approach.* Chemical Engineering Journal, 166(2), 678 – 686, 2011. ISSN 1385-8947. 13

Dignac et al., **1998**. M.F. Dignac, V. Urbain, D. Rybacki, A. Bruchet, D. Snidaro and P. Scribe. *Chemical description of extracellular polymers: Implication on activated sludge.* Water Sci. Technol., 38(8-9), 45–53, 1998. 13

Fernandez-Nieves et al., **2000**. A Fernandez-Nieves, A. Fernandex-Barbero, B. Vincent and J. Nieves. *Charge Controlled Swelling of Microgel Particles.* Macromolecules, 33(6), 2114–2118, 2000. 13

Froelund et al., **1996**. Bo Froelund, Rikke Palmgren, Kristian Keiding and Per Halkjear Nielsen. *Extraction of extracellular polymers from activated sludge using a cation exchange resin.* Water Research, 30(8), 1749 – 1758, 1996. ISSN 0043-1354. 13

Iritani et al., **2015**. Eiji Iritani, Nobuyuki Katagiri, Toshiharu Takenaka and Yuuki Yamashita. *Membrane pore blocking during cake formation in constant pressure and constant flux dead-end microfiltration of very dilute colloids.* Chemical Engineering Science, 122, 465 – 473, 2015. ISSN 0009-2509. 43, 44

Jackson and James, **1986**. Graham W. Jackson and David F. James. *The permeability of fibrous porous media.* The Canadian Journal of Chemical Engineering, 64(3), 364–374, 1986. ISSN 1939-019X. 45, 49, 50, 54

Keiding and Wybrand, **2001**. K Keiding and L Wybrand. *Remember the water - a comment on EPS colligative properties.* Water Science and Technology, 43(6), 17–23, 2001. 11, 13, 14, 19

Keiding and Rasmussen, **2003**. Kristian Keiding and Michael R. Rasmussen. *Osmotic effects in sludge dewatering.* Advances in Environmental Research, 7(3), 641–645, 2003. 13, 14, 15, 16

Legrand et al., **1998**. V Legrand, D Hourdet, R Audebert and D Snidaro. *Deswelling and flocculation of gel networks: application to sludge dewatering.* Water Research, 32(12), 3662 – 3672, 1998. ISSN 0043-1354. 16

Lin et al., **2011**. H. J. Lin, W. J. Gao, K. T. Leung and B. Q. Liao. *Characteristics of different fractions of microbial flocs and their role in membrane fouling.* Water Science and Technology, 63(2), 262–269, 2011. ISSN 0273-1223. 11

Lin et al., **2009**. H.J. Lin, K. Xie, B. Mahendran, D.M. Bagley, K.T. Leung, S.N. Liss and B.Q. Liao. *Sludge properties and their effects on membrane fouling in submerged anaerobic membrane bioreactors (SAnMBRs).* Water Research, 43(15), 3827 – 3837, 2009. ISSN 0043-1354. 11

Lin et al., **2014a**. Hongjun Lin, Meijia Zhang, Fangyuan Wang, Yiming He, Jianrong Chen, Huachang Hong, Aijun Wang and Haiying Yu. *Experimental evidence for osmotic pressure-induced fouling in a membrane bioreactor.* Bioresource Technology, 158, 119 – 126, 2014. ISSN 0960-8524. 11, 13, 50, 55, 56

Lin et al., **2014b**. Hongjun Lin, Meijia Zhang, Fangyuan Wang, Fangang Meng, Bao-Qiang Liao, Huachang Hong, Jianrong Chen and Weijue Gao. *A critical review of extracellular polymeric substances (EPSs) in membrane bioreactors: Characteristics, roles in membrane fouling and control strategies.* Journal of Membrane Science, 460, 110 – 125, 2014. ISSN 0376-7388. 12, 13

Liu and Fang, **2003**. Yan Liu and Herbert H. P. Fang. *Influences of Extracellular Polymeric Substances (EPS) on Flocculation, Settling, and Dewatering of Activated Sludge.* Critical Reviews in Environmental Science and Technology, 33(3), 237–273, 2003. 13

Lorenzen et al., **2014**. Soeren Lorenzen, Mogens Hinge, Morten Lykkegaard Christensen and Kristian Keiding. *Filtration of core-shell colloids in studying the dewatering properties of water-swollen materials.* Chemical Engineering Science, 116, 558 – 566, 2014. ISSN 0009-2509. 20

Pauling and Brockway, **1937**. Linus Pauling and L. O. Brockway. *Carbon-Carbon Bond Distances. The Electron Diffraction Investigation of Ethane, Propane, Isobutane, Neopentane, Cyclopropane, Cyclopentane, Cyclohexane, Allene, Ethylene, Isobutene, Tetramethylethylene, Mesitylene, and Hexamethylbenzene. Revised Values of Covalent Radii.* Journal of the American Chemical Society, 59(7), 1223–1236, 1937. 35

Ping Chu and Li, **2005**. Hiu Ping Chu and Xiao-yan Li. *Membrane fouling in a membrane bioreactor (MBR) Sludge cake formation and fouling characteristics.* Biotechnology and Bioengineering, 90(3), 323–331, 2005. ISSN 1097-0290. 11

Pokhrel et al., **2000**. Megh Raj Pokhrel, and Stefan H. Bossmann. *Synthesis, Characterization, and First Application of High Molecular Weight Polyacrylic Acid Derivatives Possessing Perfluorinated Side Chains and Chemically Linked Pyrene Labels.* The Journal of Physical Chemistry B, 104(10), 2215–2223, 2000. 36

Reshes et al., **2008**. Galina Reshes, Sharon Vanounou, Itzhak Fishov and Mario Feingold. *Cell Shape Dynamics in Escherichia coli*. Biophysical Journal, 94(1), 251 – 264, 2008. ISSN 0006-3495. 32

Sheng et al., **2010**. Guo-Ping Sheng, Han-Qing Yu and Xiao-Yan Li. *Extracellular polymeric substances (EPS) of microbial aggregates in biological wastewater treatment systems: A review*. Biotechnology Advances, 28(6), 882 – 894, 2010. ISSN 0734-9750. 13

Tiller and Horng, **1983**. Frank M. Tiller and Liou-Liang Horng. *Hydraulic deliquoring of compressible filter cakes. Part 1: Reverse flow in filter presses*. AIChE Journal, 29(2), 297–305, 1983. ISSN 1547-5905. 43, 52

Wang et al., **2007**. Xiao-Mao Wang, Xiao-Yan Li and Xia Huang. *Membrane fouling in a submerged membrane bioreactor (SMBR) Characterisation of the sludge cake and its high filtration resistance*. Separation and Purification Technology, 52(3), 439 – 445, 2007. ISSN 1383-5866. 11

Weiss and Silberberg. N. Weiss and A. Silberberg. *Permeability as a Means to Study the Structure of Gels*. pages 69–79. 45, 48

Yin et al., **2009**. De-Wei Yin, Monica Olvera de la Cruz and Juan J. de Pablo. *Swelling and collapse of polyelectrolyte gels in equilibrium with monovalent and divalent electrolyte solutions*. The Journal of Chemical Physics, 131(19):194907, 2009. 49

Yoon, **2013**. Seong-Hoon Yoon. *Comment on "A new insight into membrane fouling mechanism in submerged membrane bioreactor: Osmotic pressure during cake layer filtration"*. Water Research, 47(13), 4788 – 4789, 2013. ISSN 0043-1354. 14

Zhang et al., **2013**. Meijia Zhang, Wei Peng, Jianrong Chen, Yiming He, Linxian Ding, Aijun Wang, Hongjun Lin, Huachang Hong, Ye Zhang and Haiying Yu. *A new insight into membrane fouling mechanism in submerged membrane bioreactor Osmotic pressure during cake layer filtration*. Water Research, 47(8), 2777 – 2786, 2013. ISSN 0043-1354. 11, 13, 14, 15

Appendix A Piston system program

A.1 Data naming system

The data was named by the following structure:
a-bb-ccc-ddd
Where a is 1,2 or 3, which respectively represent if the measurements is a pure water flux, the PAA deposition experiment or a measurement of flux through the filter cake. bb is the two-digit experiment series ID. ccc is the sodium chloride concentration in decigrams per liter (ie. 040 is 4 $\frac{g}{l}$). Finally ddd is the number of the experiment within the experiment series. As an example, the following ID:
2-08-160-007
refers to the PAA deposition experiment in the experiment series ID of 08 at a sodium chloride concentration of 16 $\frac{g}{l}$, with the current filtration being number 7 in the experiment series.

A.2 Data example

Following is the beginning of the dataset for data point 1-02-060-004:

```
1  Date and time: 07/01/201613:30:10
2  Applied pressure: 0.3
3  Sampling rate: 3
4  Stepmotor set to: HIGH
5  Cylinder diameter: 5
6  Operator name: Jakob Pedersen
7  Original filename: C:\Documents and Settings\filtreringspc\Skrivebord\Jakob\new
       \1-02-060-004
8  Notes:
9  6g/l mem#8
10
11
12 Time ; Pextern (bar) ; Pliquid (bar) ; Possition (mm) ; Temperature (C) ;
       Ppiston face (bar)
13 3.57500009704381;0.284226131968474;0.236626919409804;2.23518432104526;-18.1948564329646;-2
14 6.57999976538122;0.187798425731433;0.227115249322757;5.46430237984134;-18.1948564329646;-2
15 9.58399989176542;0.128697573521635;0.217999898822669;8.88474101726552;-18.1948564329646;-2
16 12.5880000181496;0.156692714042066;0.216810940061788;12.4218385440971;-18.1948564329646;-2
```

The data that was used for further calculations were the time and the piston position, which for this data has been illustrated in **Figure A.1**.

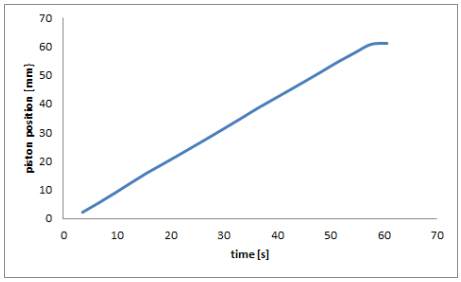

Figure A.1: *piston position plotted as a function of time for experiment 1-02-060-004*

A.3 Data program

```
function []=Masterfunction()
transformdata()
getdatasort()
Metadata()
end
```

```
function []=transformdata()
%disp('File shuffling initiated')
files=dir('Raw data');
antal=size(files,1);

for i=3:(antal)
    filename=files(i).name;
    datatype=textscan(filename,'%1.s %*s');
    membrane=textscan(filename,'%*2.s %2.s %*s');
    csalt=textscan(filename,'%*5.s %3.s %*s');
    expnr=textscan(filename,'%*9.s %3.s %*s');

    newfilename=strcat(char(membrane{1}),'-',char(expnr{1}),'-',char(datatype
        {1}),'-',char(csalt{1}));

    copyfile(strcat('Raw data\',filename),strcat('Datafiles\','',newfilename,'.
        txt'),'f')

end

disp(['File shuffling completed for ' mat2str(antal-2) ' entries!'])
end
```

```
function getdatasort()
disp('Data aquisition initiated!')
datasource='Datafiles/';
plotdir='Plots/';
outputdir='Resistances/';

files=dir(strcat(datasource,'*.txt'));

outputfile=0; %cell2mat(textscan(strcat(files(1).name),'%2.c %*s')); %initial
    outputfile

ii=1;
begintime=now;
```

```
%fopen(outputfile,'w'); %til at overskrive

    for i=1:1:size(files,1)
        if str2double(outputfile) ~= str2double(cell2mat(textscan(strcat(files(i).name),'%2.c %*s'))) %laver ny outputfil afhaengig af forsoegsnummeret
            outputfile=cell2mat(textscan(strcat(files(i).name),'%2.c %*s'));
            fclose all;
            outputlocation=strcat(outputdir,outputfile,'.txt');
            FID=fopen(outputlocation,'w');
            fprintf(FID,'%s %s %s %s %s %s %s %s %s %s \r\n','expNR','dagen','expTYPE','Pressure','R','R2','fitrange','saltC','rslope','roffset');
        end
        Fileimportersort(datasource,strcat(files(i).name),outputlocation,plotdir) %her du skal sortere efter datatype!
        currenttime=now;

        if i==(5*ii)
            elapsedtime=(currenttime-begintime)*100000/1.15; %in seconds ca.
            progress=i/(size(files,1));
            rateofcalc=elapsedtime/i;
            estremainingtime=(size(files,1)-i)*rateofcalc;

            disp([mat2str(round(estremainingtime)) ' seconds left, and ' mat2str(round(progress*100)) '% complete']);
            ii=ii+1;
        end
    end

fclose all;
close all;
disp(['  ']);
disp(['Data gathered for ' mat2str(i) ' entries!'])
disp(['Elapsed time: ' mat2str(round(elapsedtime)) ' seconds'])
end
```

```
function getdatasort()
disp('Data aquisition initiated!')
datasource='Datafiles/';
plotdir='Plots/';
outputdir='Resistances/';

files=dir(strcat(datasource,'*.txt'));

outputfile=0; %cell2mat(textscan(strcat(files(1).name),'%2.c %*s')); %initial outputfile

ii=1;
begintime=now;
%fopen(outputfile,'w'); %til at overskrive

    for i=1:1:size(files,1)
        if str2double(outputfile) ~= str2double(cell2mat(textscan(strcat(files(i).name),'%2.c %*s'))) %laver ny outputfil afhaengig af forsoegsnummeret
            outputfile=cell2mat(textscan(strcat(files(i).name),'%2.c %*s'));
            fclose all;
```

```
19                outputlocation=strcat(outputdir,outputfile,'.txt');
20                FID=fopen(outputlocation,'w');
21                fprintf(FID,'%s %s %s %s %s %s %s %s %s %s \r\n','expNR','dagen','
                      expTYPE','Pressure','R','R2','fitrange','saltC','rslope','roffset
                      ');
22            end
23            Fileimportersort(datasource,strcat(files(i).name),outputlocation,plotdir
                  ) %her du skal sortere efter datatype!
24            currenttime=now;
25
26            if i==(5*ii)
27                elapsedtime=(currenttime-begintime)*100000/1.15; %in seconds ca.
28                progress=i/(size(files,1));
29                rateofcalc=elapsedtime/i;
30                estremainingtime=(size(files,1)-i)*rateofcalc;
31
32                disp([mat2str(round(estremainingtime)) ' seconds left, and ' mat2str
                      (round(progress*100)) '% complete']);
33                ii=ii+1;
34            end
35        end
36
37    fclose all;
38    close all;
39    disp(['  ']);
40    disp(['Data gathered for ' mat2str(i) ' entries!'])
41    disp(['Elapsed time: ' mat2str(round(elapsedtime)) ' seconds'])
42    end
```

```
1   function [] = Fileimportersort( datasource,file,outputfile,plotdir )
2
3   %Directories
4   plotfile=textscan(file,'%12.s %*s');
5
6
7   %SETUP
8   format long
9   Radius=2.5/100;                 %m cylinder radius
10  Viscosity=0.001/(10^5);         %bar*s (/10^5 for bar*s). PAA paavirker viscosity
        dog!!
11  Area=Radius^2*pi;               %m2
12
13
14  %AQUIRE FILENAME INFO
15  [memID,expNR,expTYPE,saltC] = filenameinfo(file); %gemt som strings
16
17
18
19  %AQUIRE HEADERLINES INFO
20  FID=fopen(strcat(datasource,file),'rt');
21  [dagen,datoen,klokken,Pressure]=getheaderinfo(FID);
22  fclose(FID);
23
24
25  %LOADING DATASET
26  Headerlines=12;
27  FID=fopen(strcat(datasource,file),'rt');
```

```
28 Datacell=textscan(FID,'%f %f %f %f %*f %*f','HeaderLines',Headerlines,'Delimiter
       ',';');
29 fclose(FID);
30 Datacell=cell2mat(Datacell);
31
32
33
34
35 %DATA TREATMENT: DETERMINING dV/dT
36 cut_off=2;                                          %antal data der skal
       fjernes fra slut i datasaettet
37 datarange=size(Datacell,1)-cut_off-1;               %-1 fordi flux!;
38 dvdt=[zeros(datarange,1)];                          %m3/sek
39 for i=1:1:datarange                                 %-1 fordi der er 3
       trapper i en 4 etagers bygning!
40     dv=(Datacell((i+1),4)-Datacell(i,4))*Area/1000;  %m3
41     dt=Datacell((i+1),1)-Datacell(i,1);              %sek
42     dvdt(i)=dv/dt;
43 end
44
45
46
47
48
49 %RAW DATA
50 Datacell((datarange+1):(size(Datacell,1)),:)=[];
51
52 tid=Datacell(:,1);          %sek
53 pext=Datacell(:,2);         %bar
54 pliq=Datacell(:,3);         %bar
55 pos=Datacell(:,4)/1000;     %m
56 vol=pos*Area;               %m3
57 dvdt=dvdt;                  %m3/sek
58 fluxms=dvdt/Area;           %m/sek
59 fluxlmh=fluxms*1000*60^2;   %LMH
60
61
62
63
64 %ISOLATION OF FILTRATION DATA      (virker ikke hvis dataset er lille (<10))
65 ActiveScanRange=3; %den fraktion af i som der sammenlignes med
66 fitsensitivity=20;          %i procent (af max dvdt)
67 [fitrange]=getfitrange(datarange,ActiveScanRange,fitsensitivity,dvdt);
68
69
70
71
72 %FILTRATION DATA
73 ftid=tid(1:fitrange);           %sek
74 fpext=pext(1:fitrange);         %bar
75 fpliq=pliq(1:fitrange);         %bar
76 fpos=pos(1:fitrange);           %m
77 fvol=vol(1:fitrange);           %m3
78 fdvdt=dvdt(1:fitrange);         %m3/sek
79 ffluxms=fluxms(1:fitrange);     %m/s
80 ffluxlmh=fluxlmh(1:fitrange);   %lmh
81
82
```

```
83
84
85
86 %LINEAR FITTING                of (tid,vol)
87 [R2,rslope,roffset]=regression(ftid',fvol'); %bedre metode. kraever rette matrix
       dimensioner
88 lvol=ftid*rslope+roffset; %linfit(1)=b & linfit(2)=a
89
90
91
92 %PLOTTING
93 hold off
94 plot(tid,vol)
95 hold on
96 plot(ftid,fvol,'red','LineWidth',2)
97 plot(ftid,lvol,'black','LineWidth',1.5)
98 hold off
99
100
101 R=Area*Pressure/(Viscosity*rslope);
102 % disp(num2str(rslope))
103 % disp(num2str(R))
104 % disp(num2str(Area))
105 % disp(num2str(Pressure))
106 % disp(num2str(Viscosity))
107
108 % display(Pressure)
109 % display(R)
110
111 %DATA SAVING
112 % fileID=fopen(outputfile,'a+');
113 % fprintf(fileID,'%s %s %s %f %f %f %f \r\n',datoen,klokken,file,Pressure,R,R2,
       fitrange);
114 % fclose('all');
115 fileID=fopen(outputfile,'a+');
116
117 fprintf(fileID,'%f %f %f %f %f %f %f %f %.20f %.10f \r\n',str2double(expNR),
       str2double(dagen),str2double(expTYPE),Pressure,R,R2,fitrange,str2double(saltC
       ),rslope,roffset);
118 fclose('all');
119
120 %PLOT SAVING
121 saveas(gcf,strcat(plotdir,char(plotfile{1})),'png')
122
123 end
124
125
126
127 function [memID,expNR,expTYPE,saltC] = filenameinfo(file)
128 memID=cell2mat(textscan(file,'%2.c %*s'));
129 expNR=cell2mat(textscan(file,'%*3.c %3.c %*s'));
130 expTYPE=cell2mat(textscan(file,'%*7.c %1.c %*s'));
131 saltC=cell2mat(textscan(file,'%*9.c %3.c %*s'));
132 end
133
134
135
136 function [dagen, datoen, klokken, Pressure] = getheaderinfo( FID )
```

```
137 tline=fgets(FID); %evt. goer dette smartere.
138 Datescan=cell2mat(textscan(tline,'%14.*c␣%f␣%f␣%4.f␣%f␣%f␣%f','Delimiter',':␣/'
    ));
139 dagen=mat2str(Datescan(1));
140 datoen=strcat(mat2str(Datescan(1)),':',mat2str(Datescan(2)),':',mat2str(Datescan
    (3)));
141 klokken=strcat(mat2str(Datescan(4)),':',mat2str(Datescan(5)),':',mat2str(
    Datescan(6)));
142 tline=fgets(FID);
143 Pressure=cell2mat(textscan(tline,'%*s␣%f','Delimiter',':')); %bar
144 end
145
146
147
148 function [fitrange]=getfitrange( datarange,ActiveScanRange,fitsensitivity,dvdt )
149     for i=1:1:datarange
150     xmin=round(i/ActiveScanRange*(ActiveScanRange-1));
151     ymax=max(dvdt(xmin:i));
152     ycurrent=dvdt(i);
153         if ycurrent<ymax*fitsensitivity/100
154             fitrange=i-3; %-3 for at komme til 'lige' stykke
155             break
156         else fitrange=datarange;
157         end
158     end
159 end
```

```
1  function [] = Metadata()
2  folder='Resistances/';
3  plotfolder='Resistanceplots/';
4  outputfile='Resistanceplots/Masterdata.txt';
5  fileID=fopen(outputfile,'w');
6  fprintf(fileID,'%s␣%s␣%s␣%s␣%s␣%s␣%s␣%s␣%s␣\r\n','expID','saltC','Rmavg','
       averageRtotal','maxRtotaldev','minRtotaldev','averagePitotal','maxPitotaldev'
       ,'minPitotaldev');
7
8  files=dir(folder);
9  antal=size(files,1);
10 Resistances=[];
11 maxResistancesdev=[];
12 minResistancesdev=[];
13 Osmopressures=[];
14 maxOsmopressuresdev=[];
15 minOsmopressuresdev=[];
16
17 Saltkonc=[];
18
19 for i=3:(antal)
20     FID=fopen(strcat(folder,files(i).name));
21     %tline=fgets(FID)
22     %textscan(FID,'%f')
23     Datacell=textscan(FID,'%f␣%f␣%f␣%f␣%f␣%f␣%f␣%f␣%f','HeaderLines',1);
24
25     expnr=Datacell{1};
26     Pressure=Datacell{4}; %FUUUCK DET FUCKING 3 TAL ARRRGHHHH
27     Rtotal=Datacell{5};
28     Date=Datacell{2};
29     exptype=Datacell{3};
```

```
30      saltC=Datacell{8};
31      saltC=saltC(1,1)/10; %g/l
32      slope=Datacell{9};
33      %invslope=1./slope; %saadan man inverterer matrix
34
35      expID=(textscan(files(i).name,'%2.s_%*s'));
36      expID=char(expID{1});
37
38
39
40      waterflux=[];
41      waternr=[];
42      deposition=[];
43      deponr=[];
44      cakeflux=[];
45      cakenr=[];
46      Rmarray=[];
47
48      for ii=1:size(exptype)
49          if exptype(ii)==1
50              waterflux=[Rtotal(ii) waterflux];
51              waternr=[expnr(ii) waternr];
52              if Pressure(ii)>0.25
53                  Rmarray=[Rtotal(ii) Rmarray];
54                  Rmend=expnr(ii);
55              end
56
57          end
58          if exptype(ii)==2
59              deposition=[Rtotal(ii) deposition];
60              deponr=[expnr(ii) deponr];
61              cakefluxdaybegin=expnr(ii)+1; %bruges til at finde avg range
62          end
63          if exptype(ii)==3
64              cakeflux=[Rtotal(ii) cakeflux];
65              cakenr=[expnr(ii) cakenr];
66
67          end
68
69      end
70
71
72      %For osmotic fit determination (under assumption that Rc=0 --> Rt=Rm
73      Radius=2.5/100; %m
74      Area=Radius^2*pi; %m2
75      Viscosity=0.001/(10^5);
76      %pprs=Pressure./slope;
77      Rmavg=mean(Rmarray);
78      Piest=Pressure-slope*(Viscosity*Rmavg/Area);
79
80      %konst=Area/Viscosity; %Used for Rtotal test of calc.
81      %Rtotaltest=konst*pprs;%Used for Rtotal test of calc.
82      %osmotic fit determination end
83
84
85
86
87
```

```
88
89
90
91      Daybreaks=[];
92      Dayavg=[];
93
94      for ii=1:(size(Date)-1) %bestemmelse af dagsskift, samt ranges af relevant
            data i hver dag
95          currentdate=Date(ii);
96          nextdate=Date(ii+1);
97          if currentdate ~= nextdate
98              Daybreaks=[Daybreaks expnr(ii)];
99              Dayavg=[Dayavg; cakefluxdaybegin expnr(ii)];
100             cakefluxdaybegin=expnr(ii)+1;
101         end
102     end
103
104     Dayavg=[Dayavg; cakefluxdaybegin size(expnr,1)];
105     %her er avg roderi
106     AVGRt=[];
107     MAXRt=[];
108     MINRt=[];
109
110     AVGPi=[];
111     MAXPi=[];
112     MINPi=[];
113
114
115     for ii=1:1:size(Dayavg,1) %kun de foerste 2 dage
116         avgstart=Dayavg(ii,2)-(Dayavg(ii,2)-Dayavg(ii,1))/4; %kun den sidste 4-
                del af hver dags maalinger
117         AVGRt=[AVGRt mean(Rtotal(round(avgstart):Dayavg(ii,2)))];
118         MAXRt=[MAXRt max(Rtotal(round(avgstart):Dayavg(ii,2)))];
119         MINRt=[MINRt min(Rtotal(round(avgstart):Dayavg(ii,2)))];
120
121         AVGPi=[AVGPi mean(Piest(round(avgstart):Dayavg(ii,2)))];
122         MAXPi=[MAXPi max(Piest(round(avgstart):Dayavg(ii,2)))];
123         MINPi=[MINPi min(Piest(round(avgstart):Dayavg(ii,2)))];
124     end
125
126     if size(AVGRt,2)>2 %vist fordi der var nogle issues med at der kom data fra
            de senere dage med alligevel
127       AVGRt(3:(size(AVGRt,2)))=[];
128       MAXRt(3:(size(MAXRt,2)))=[];
129       MINRt(3:(size(MINRt,2)))=[];
130
131       AVGPi(3:(size(AVGPi,2)))=[];
132       MAXPi(3:(size(MAXPi,2)))=[];
133       MINPi(3:(size(MINPi,2)))=[];
134     end
135
136     averageRtotal=mean(AVGRt);
137     maxRtotal=max(MAXRt);
138     minRtotal=min(MINRt);
139
140     averagePitotal=mean(AVGPi);
141     maxPitotal=max(MAXPi);
142     minPitotal=min(MINPi);
```

```
143
144     avgxRt=[0 size(expnr,1)];
145     avgyRt=[averageRtotal averageRtotal];
146     maxxRt=[0 size(expnr,1)];
147     maxyRt=[maxRtotal maxRtotal];
148     minxRt=[0 size(expnr,1)];
149     minyRt=[minRtotal minRtotal];
150
151     avgxPi=[0 size(expnr,1)];
152     avgyPi=[averagePitotal averagePitotal];
153     maxxPi=[0 size(expnr,1)];
154     maxyPi=[maxPitotal maxPitotal];
155     minxPi=[0 size(expnr,1)];
156     minyPi=[minPitotal minPitotal];
157
158     Rmy=[Rmavg Rmavg];
159     Rmx=[0 Rmend];
160
161     %avg roderi
162
163     maxR=max(Rtotal)*1.1;
164     Dateline=[0; maxR];
165     Daybreaks=[Daybreaks; Daybreaks]+0.5;
166
167
168 %       plot(expnr,Rtotal,'s')
169     figure(1)
170
171     plot(waternr,waterflux,'blue.','MarkerSize',13)
172     hold on
173     plot(deponr,deposition,'red.','MarkerSize',13)
174     plot(cakenr,cakeflux,'black.','MarkerSize',13)
175     plot(avgxRt,avgyRt,'blue')
176     for ii=1:size(Daybreaks,2)
177         plot(Daybreaks(:,ii),Dateline,'black')
178     end
179     plot(maxxRt,maxyRt,'cyan')
180     plot(minxRt,minyRt,'cyan')
181     %plot(Rmx,Rmy,'black') %waterflux avg
182
183
184     hold off
185
186     xlabel('exp nr') % label x-axis
187     ylabel('Total filtration resistance') % label left y-axis
188     title(strcat('NaCl konc  ',' ',num2str(saltC),' g/l'))
189     legend('Waterflux','PAA450kDa deposition','Cake filtration','"Plateau" Rt','
            Overnight equilibrium')
190
191     saveas(gcf,strcat(plotfolder,'Rtotal ',expID),'png');
192
193     figure(2)
194     plot(expnr,Piest,'.')
195     hold on
196     plot(avgxPi,avgyPi,'blue')
197     plot(maxxPi,maxyPi,'green')
198     plot(minxPi,minyPi,'red')
199
```

```
200     maxPi=max(Piest)*1.1;
201     Dateline=[0; maxPi];
202     for ii=1:size(Daybreaks,2)
203         plot(Daybreaks(:,ii),Dateline,'black')
204     end
205     hold off
206
207     hold off
208     saveas(gcf,strcat(plotfolder,'Piest ',expID),'png');
209
210
211
212     maxRtotaldev=maxRtotal-averageRtotal;
213     minRtotaldev=averageRtotal-minRtotal;
214
215     maxPitotaldev=maxPitotal-averagePitotal;
216     minPitotaldev=averagePitotal-minPitotal;
217
218     Resistances=[averageRtotal Resistances];
219     maxResistancesdev=[maxRtotaldev maxResistancesdev];
220     minResistancesdev=[minRtotaldev minResistancesdev];
221
222     Osmopressures=[averagePitotal Osmopressures];
223     maxOsmopressuresdev=[maxPitotaldev maxOsmopressuresdev];
224     minOsmopressuresdev=[minPitotaldev minOsmopressuresdev];
225
226
227     Saltkonc=[saltC Saltkonc];
228     fprintf(fileID,'%s %f %f %f %f %f %f %f %f \r\n',expID,saltC,Rmavg,
            averageRtotal,maxRtotaldev,minRtotaldev,averagePitotal,maxPitotaldev,
            minPitotaldev);
229
230     %fclose all;
231 end
232 %maxResistances=maxResistances-Resistances;
233 %minResistances=Resistances-minResistances;
234 figure(3)
235 errorbar(Saltkonc,Resistances,maxResistancesdev,minResistancesdev,'.');
236 %plot(Saltkonc,Resistances,'.','MarkerSize',13)
237 axis([0,max(Saltkonc)*1.2,0,max(Resistances)*1.2])
238 xlabel('Salt conc. [g/l]') % label x-axis
239 ylabel('Total filtration resistance') % label left y-axis
240 saveas(gcf,strcat(plotfolder,'Masterplot'),'png');
241
242 figure(4)
243 errorbar(Saltkonc,Osmopressures,maxOsmopressuresdev,minOsmopressuresdev,'.');
244 axis([0,max(Saltkonc)*1.2,0,max(Osmopressures)*1.2])
245 xlabel('Salt conc. [g/l]') % label x-axis
246 ylabel('Estimeret osmotisk tryk i kage') % label left y-axis
247 saveas(gcf,strcat(plotfolder,'Masterplot2'),'png');
248
249 fclose all;
250 close all
251 end
```

Appendix B Continuous system program

B.1 Data example

The following is the beginning of a dataset.

```
Her er en data fil fra: 04-04-2016 15:21:30
Der er 1sec mellem hver maaling.
Angiv Forsoegsnoter her


Tid ; Stabilitet ; Masse ; Enhed
0,0450001331046224;S S ;      348.43 ;  g
1,05299984570593;S S ;      348.43 ;  g
2,06100018694997;S S ;      348.42 ;  g
3,08500011451542;S S ;      348.42 ;  g
```

The data was analysed individually for each experiment using the data handling script in **Appendix B.2**.

B.2 Data program

```
function [] = sv( name, filename)
visc=0.001; %Pa*s
hvand=1.40; %m
dvand=1000; %kg/m3
dP=hvand*10000; %Pa
radius=4.3/100/2; %m
A=radius^2*pi; %m2




smoothrange=100; %hele dette er lavet saaledes jeg kan kigge paa MEGET lave flux (Rt>10^13)
cutval=10;
smoothvaegten=21;

FID=fopen(filename);
Datacell=textscan(FID,'%s %*s %f %*s','HeaderLines',6,'Delimiter',';');
%Datacell=textscan(FID,'%f %*s %f %*s','HeaderLines',6,'Delimiter',';')
tid=Datacell{1};
tid=strrep(tid,',','.');
% for i=2:size(tid,1) %for locating lines of error in data (errors from the datalogger).
%     if str2double(tid(i))>str2double(tid(i-1))
%
%     else
%         i
%     end
% end

tid=cellfun(@str2double,tid); %sek
vaegt=Datacell{2}; %g
% for 2mg PAA3MDa
% for i=1:1:size(vaegt,1)-1
```

```
32 %       tid(i)
33 %       vaegt(i)
34 %       if vaegt(i)>0
35 %       else
36 %           vaegt(i)=[];
37 %           tid(i)=[];
38 %           i=i-1;
39 %       end
40 % end
41 %%
42 vaegt=smooth(vaegt,smoothvaegten); %test smoothing Deactiveret, giver nogle bugs
       .
43 vol=vaegt*(1/(1000*dvand)); %m3
44
45 %differentier
46 dVdt=zeros((size(tid,1)),1);
47 for i=1:1:size(tid,1)-2 %-1 pga numerisk differentiering
48     dV=vol(i+1)-vol(i);
49     dt=tid(i+1)-tid(i);
50     dVdt(i)=dV/dt; %m3/s
51 end
52
53
54 %fjern kanter, summer vol og fyld hullerne (lin reg v. vol og kopiering af
55 %data v. dVdt
56
57
58 dVdtcut=dVdt; %m3/s
59 dropstate=0;
60 volsum=zeros((size(tid,1)),1);
61 precurrentsum=0;
62 currentsum=0;
63 sumstart=0;
64 dropstart=0;
65 dropstop=0;
66 linregendsum=0;
67
68 for i=1+cutval:1:size(tid,1)-cutval
69     if dropstate==0
70         %volsum(i)=vol(i)+(currentsum-sumstart)+(currentsum-precurrentsum)/20*(
               dropstop-dropstart); %precurrentsum er simple linear reg.
71         volsum(i)=vol(i)+(linregendsum-sumstart);
72     end
73
74     if dVdt(i)<0 && dVdt(i-1)>0 && dropstate==0 %hvis vi er i filtration mode,
           og flux bliver negativ
75         precurrentsum=volsum(i-cutval);
76         currentsum=volsum(i-1); %aendret -1 til -cutval
77         dropstate=1;
78         dropstart=i-cutval;
79
80     end
81     if dVdt(i)>0 && dVdt(i-1)<0 && dropstate==1 %hvis vi er i bucket-empty mode
           og flux bliver positiv
82         i=i+cutval; %saet i til at vaere +cutval over flux begynder igen
83         dropstop=i; %punktet vi siger er tilbage til normal flux
84         sumstart=vol(dropstop); %sumvaerdien vi bruger til at regne differencen
               i vol under dropstate=1
```

```
85
86          if i>(10*cutval) %undgaar at trigger v. start af datasaet (skaber bugs)
87              dVdtcut(dropstart:dropstop)=dVdtcut(dropstart-(dropstop-dropstart):
                    dropstop-(dropstop-dropstart)); %dVdtcut((dropstart-(dropstart-
                    dropstop)):dropstart);
88          end
89
90          for ii=dropstart:1:dropstop %linear reg af vol i droparea.
91              volsum(ii)=volsum(ii-1)+(currentsum-precurrentsum)/20;%-0.0000001;
92             % volsum(ii)=currentsum+(currentsum-precurrentsum)/20*(ii-dropstart);
93             linregendsum=volsum(ii);
94          end
95
96          dropstate=0;
97      end
98  end
99
100
101 volsum=volsum-volsum(cutval+1);
102 flux=dVdtcut/A; %m/s
103
104 Rt=zeros((size(tid,1)),1);
105 for i=1:1:size(tid,1) %i=1+cutval*10:1:size(tid,1)-cutval
106     if flux(i)>2*10^-6 %test for at fjerne high points.
107     Rt(i)=dP/(visc*flux(i)); %1/m
108     end
109 end
110
111
112 cutstart=0+cutval*5; %cutning af data, for at fjerne enderne. skal goere for
        alle data inden plotning.
113 cutslut=size(tid,1)-cutval*5;
114
115 dVdt=dVdt(cutstart:cutslut);
116 tid=tid(cutstart:cutslut);
117 volsum=volsum(cutstart:cutslut);
118 flux=flux(cutstart:cutslut);
119 Rt=Rt(cutstart:cutslut);
120 vol=vol(cutstart:cutslut);
121
122
123 dVdtcut=[];
124 for i=1:1:(size(tid,1)/smoothrange-1)
125     dVdtcut(i)=sum(dVdt((1+(i-1)*smoothrange):(i*smoothrange)));
126     tidcut(i)=mean(tid((1+(i-1)*smoothrange):(i*smoothrange)));
127     fluxcut(i)=mean(flux((1+(i-1)*smoothrange):(i*smoothrange)));
128     volsumcut(i)=mean(volsum((1+(i-1)*smoothrange):(i*smoothrange)));
129     if dP/(visc*fluxcut(i))>0
130         Rtcut(i)=dP/(visc*fluxcut(i)); %1/m
131     else
132         Rtcut(i)=Rtcut(i-1);
133     end
134
135
136
137 end
138
139 %% %for 1,5mg PAA
```

```
% xcount=1;
% trig=0;
% for i=1:1:(size(tid,1)/smoothrange-1)
%     if tidcut(i)>1.49*10^5 && tidcut(i)<1.59*10^5
%         if trig==0
%             xstart=i;
%         end
%         xcount=xcount+1;
%         trig=1;
%     end
%
%         %fluxcut(i)=[];
% end
% %         volsumcut(xstart:xstart+xcount)=[];
% %         Rtcut(xstart:xstart+xcount)=[];
% %         tidcut(xstart:xstart+xcount)=[];
% xstart;
% xcount;
% size(tid,1)/smoothrange-1;
% volsumcutdrop=16.8*10^-3 %volsum(xstart-1)-volsum(xstart+xcount+1)
% i=0;
% for i=(735+xcount):1:1654
%     volsumcut(i)=volsumcut(i)-volsumcutdrop;
% end
%%
figure(1)
plot(tidcut,volsumcut);
xlabel('tid [s]')
ylabel('Vpermeate [m3]')

figure(2)
plot(volsumcut,Rtcut,'s','MarkerSize',2);
xlabel('Vpermeate [m3]')
ylabel('Rt [1/m]')
%axis([0 max(volsumcut) 0 6*10^13]);


figure(3)
plot(tidcut,Rtcut);
xlabel('tid [s]')
ylabel('Rt [1/m]')

figure(4)
plot(tid,vol);
xlabel('tid [s]')
ylabel('vol [m3]')

figure(5)
plot(tidcut,fluxcut);
xlabel('tid [s]')
ylabel('flux [m/s]')

scnsize = get(0,'ScreenSize');
pos1 = [3*scnsize(3)/4,scnsize(2)+40,scnsize(3)/4,scnsize(4)/2-40];
%pos2 = [scnsize(3)/2,scnsize(4)/2,scnsize(3)/4,scnsize(4)/2];
pos2 = [scnsize(3)/2,scnsize(4)/2,scnsize(3)/2,scnsize(4)/2];
pos3 = [scnsize(3)/2,scnsize(2)+40,scnsize(3)/4,scnsize(4)/2-40];
%pos4 = [3*scnsize(3)/4,scnsize(4)/2,scnsize(3)/4,scnsize(4)/2];
```

```
198
199
200 set(figure(2),'OuterPosition',pos2)
201 %set(figure(2),'OuterPosition',pos4)
202 set(figure(1),'OuterPosition',pos3)
203 set(figure(4),'OuterPosition',pos1)
204
205
206 %printfile=[distance', fliplr(Cflip')];
207 %fileID=fopen('simusave.txt','a+');
208 savematrix=[tidcut' fluxcut' Rtcut' volsumcut'];
209
210 xlswrite(strcat('Excel/',name,'.xlsx'),savematrix);
211
212
213
214 fclose all;
215
216
217
218
219
220
221 end
```

Appendix C The continuous setup

C.1 The flowmeter

The permeate drips into the bucket, which is placed on top of a weight. The weight sends data to a pc by serial communication, and the pc logs the data. The bucket is covered by a simple lid, in order to limit evaporation. A tube is inserted through the side of the bucket, and bent down into the bucket. The other end leads water into a drain.

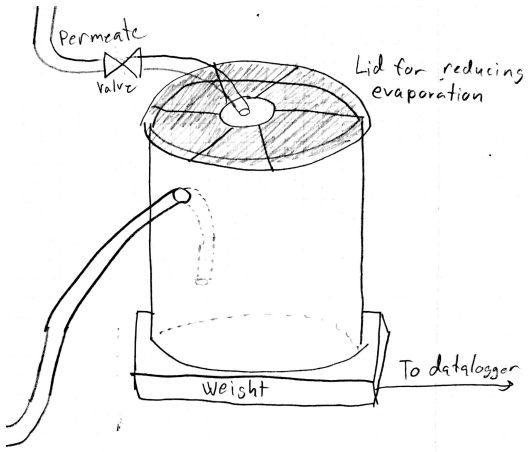

C.2 The prechamber and membrane housing

The prechamber consist of an airtight cylinder, of which an outlet leads to the membrane housing. Several valves are connected to the prechamber, one that connects to the pressure-generating cylinder with feed water, and a few others that allow for placing the filtration solutions in the prechamber.

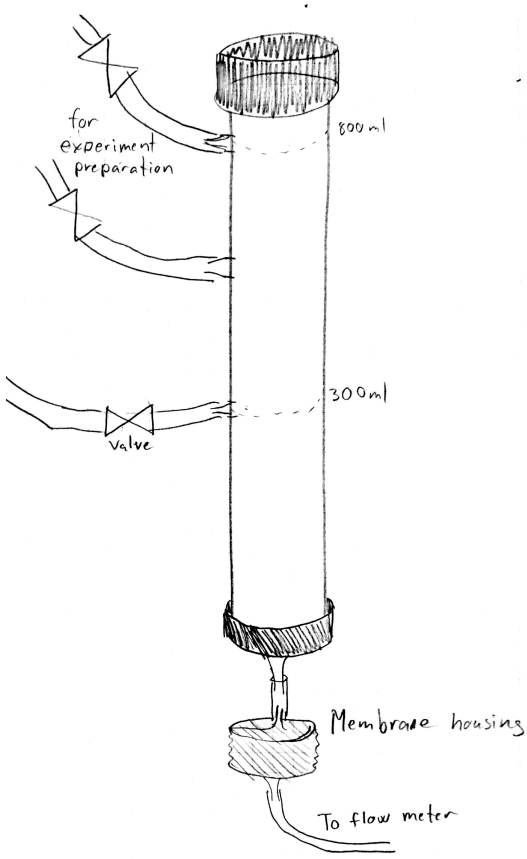

C.3 The entire setup

Here the flowmeter, prechamber and membrane housing is illustrated along with the rest of the setup. The illustrations indicate how the overflow outlets are placed, along with the pump and feed bucket.

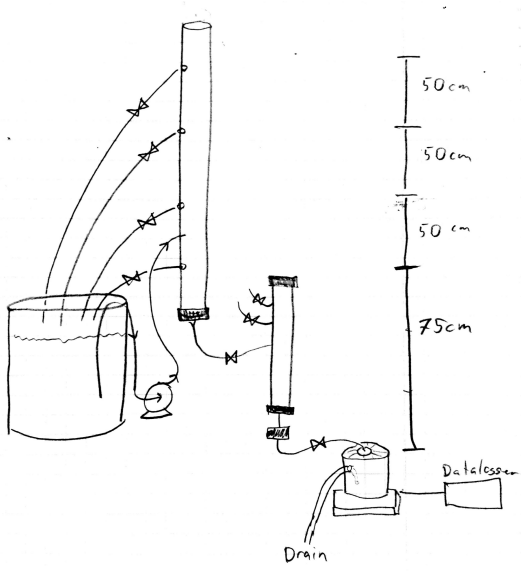

Appendix D Membrane filtration resistance

For all experiments, a 0.22 μm polyethersulfone hydrophilic membrane from Merck Millipore, catalogue number GPWP14250, was used. In order to characterize the filtration resistance of the membrane, and qualitatively check if the membranes had any significant variation therein, occasional water flux experiments were performed. The filtration resistance was found to be $(1.5 \pm 0.1) * 10^{10}\ m^{-1}$. These experiments have been performed at different filtration pressures (22 kPa and 14 kPa) and at different pH (pH 6, 9 and 11), which had no significant influence.